ABSTRACT

CHRISTIE, MEGAN ALLISON. Keratinocyte and Hepatocyte Growth Proliferation and Adhesion to Helium and Helium/Oxygen Atmospheric Pressure Plasma Treated Polyethylene Terephthalate. (Under the direction of Mohamed A. Bourham and Wendy E. Krause.)

To improve the surface properties of biomaterials, the effects of changes in surface chemistry and morphology of polyethylene terephthalate (PET) films treated with atmospheric pressure plasma were investigated as a function of cellular growth, proliferation, and adhesion. PET films were subjected to helium and helium/oxygen gas plasmas. The contact angle of the treated films decreased due to plasma etching and possible scission indicating that the surfaces become more hydrophilic. Atomic force microscopy results had a large standard error, however the surface visually showed changes in surface micro and nanoscale roughness corresponding to treatment duration. Keratinocytes were plated on the day of plasma treatment and two and five days after plasma treatment and tested half a day, one, two, three, and six days after plating. The same methodology of plating and testing was also applied to hepatocytes. Cell growth, proliferation, and adhesion were characterized via a fluorescent probe based assay and were correlated with surface chemical and nanostructural features. Both the helium and helium/oxygen plasma-treated PET had little or no effect on cell behavior for both keratinocytes and hepatocytes. The nanoscale surface changes due to the plasma surface treatment are believed to be masked by the protein adherence in the media on the surface of the PET.

KERATINOCYTE AND HEPATOCYTE GROWTH PROLIFERATION AND ADHESION TO HELIUM AND HELIUM/OXYGEN ATMOSPHERIC PRESSURE PLASMA TREATED POLYETHYLENE TEREPHTHALATE

By
MEGAN ALLISON CHRISTIE

A thesis submitted to the Graduate Faculty of North Carolina State University in partial fulfillment of the requirements for the Degree of Master of Science

BIOMEDICAL ENGINEERING
TEXTILE ENGINEERING

Raleigh, North Carolina
2005

APPROVED BY:

_____	_____
Co-chair of Advisory Committee	Co-chair of Advisory Committee

BIOGRAPHY

Megan Christie was born on February 10, 1980 and grew up in Wilmington, North Carolina. After graduating from Hoggard High School in 1998 she began undergraduate studies at North Carolina State University. She graduated with honors in 2002 with Bachelor of Science Degrees in Biological Engineering and Biomedical Engineering. Megan remained at NC State to obtain her Master of Science Degree in Textile Engineering and Biomedical Engineering.

Megan married Josh Christie on March 8, 2003 in Wilmington, North Carolina. They currently reside in Cary, North Carolina.

TABLE OF CONTENTS

LIST OF FIGURES

Page

LIST OF TABLES

I. INTRODUCTION

New materials are needed to improve the biocompatibility of implants and tissue engineered scaffolds as well as materials for bioreactors and wound healing. Most developed biomaterials have the bulk properties required for successful biomaterials, such as strength and biocompatibility, however many are lacking the surface properties needed for cellular interactions. To overcome this limitation, biomaterials can be made more suitable for cell attachment and growth through surface modification. Most current surface modification techniques result in changes to both surface morphology and chemistry. Cellular adhesion, proliferation, morphology, and differentiation are believed to be responsive to both surface topographical features and surface chemistry functionality. The relationship between these surface properties is complex as both contribute to surface wettability and possibly to protein conformational changes upon absorption. Atmospheric pressure plasma treatment of materials is one method that allows for surface modification while maintaining bulk properties. This technique is currently in use for the manufacturing of polystyrene substrates used for tissue culture. Plasma treatment of biomaterials is being investigated due to its facile procedure and sterilization of the material. Understanding how materials age and how cells react to the changes in surface chemistry is important. For example, a material used in a medical device implant may be stored at a medical facility for several months before it is implanted into a patient. In that case, the surface properties must remain stable. In other cases, such as an artificial blood vessel, the surface chemistry is important in the initial seeding of the vessel with endothelial cells and smooth muscle cells until the cells lay down their own extracellular matrix.

The role of surface chemistry and surface topography in cell growth, proliferation, and adhesion was examined. Polyethylene terephthalate (PET) films were plasma treated with pure helium and a helium/oxygen mixture for different times and keratinocytes and hepatocytes were plated on the polymer surface. The PET films were also allowed to age and the cells were again plated. The contact angle, antistatic properties, and surface morphology of the PET surface were analyzed the day of plasma treatment as well as two and five days after plasma treatment. The growth, proliferation, and adhesion of the cells on the modified surfaces were quantified 12 hours, 1, 2, 3, and 6 days after plating.

II. BACKGROUND INFORMATION

2.1 Atmospheric Plasma

Plasma, the fourth state of matter, is defined as an ionized gas containing both charged and neutral species, including free electrons, positive and/or negative ions, atoms, and molecules [1]. It is a collection of free charged particles moving in random directions that is, on average, electrically neutral and thus the plasma is a quasi-neutral medium. Interaction between a surface and plasma occurs no more than a 5 μm depth [2]. There are several atomic and molecular collisions that are responsible for the charge exchange which in turn causes a loss of hot ions. Excitation takes place when the electron populates one of the excited states (Figure 1a). When an excited atom is de-excited to the ground state and the ionization energy is released in the form of a photon, a de-excitation reaction takes place (Figure 1b). Ionization is when the electron transfers enough energy to the bound electron so that the latter will leave the atom or molecule and become free (Figure 1c). In a recombination reaction, the ion will attract a free electron to the ground state and recombine to form a neutral atom. The binding energy will be released in the form of a photon (Figure 1d). Lastly, in the case of dissociation, the formation of an energetic atom and an energetic ion will take place (Figure 1e).

a) $e^- + H \rightarrow H^* + e^-$

b) $H^* \rightarrow H + h\nu$

c) $e^- + H \rightarrow H^+ + e^- + e^-$

$e^- + H_2 \rightarrow H_2^+ + e^- + e^-$

d) $e^- + H^+ \rightarrow H + h\nu$

e) $e^- + H_2^+ \rightarrow H + H^+ + e^-$

Figure 1: Atomic and Molecular Collisions: (a) Excitation; (b) De-Excitation; (c) Ionization; (d) Recombination; (e) Dissociation

Etching is one of the key processes in plasma-aided manufacturing technology for removing materials from surfaces. The process allows for selective removal of a material so that one surface type is removed while leaving the others unaffected [3]. Etching alters both the morphology and topography of the substrate. There can be isotropic or anisotropic removal and there are four key etching processes: sputtering, chemical, reactive ion, and ion inhibitor etching (Figure 2). Sputtering (Figure 2a) occurs when the atoms of a surface are ejected due to ion bombardment. This is a very unselective process, unlike chemical etching (Figure 2b), which can be chemically selective and relatively isotropic. The plasma discharge provides a gas-phase etchant atoms or molecules and these chemically react with the surface producing gas-phase products. Reactive ion etching (Figure 2c) or ion-energy-driven etching is where the discharge supplies both energetic ions and etchant atoms. The etching products are much larger and the process has poor selectivity with high anisotropic

removal. This particular process is chemical in nature but energetic ion bombardment determine the etch rate. Ion inhibitor etching (Figure 2d) is similar to reactive ion etching, however the discharge also supplies inhibitor precursor molecules that can absorb or deposit material on the substrate.

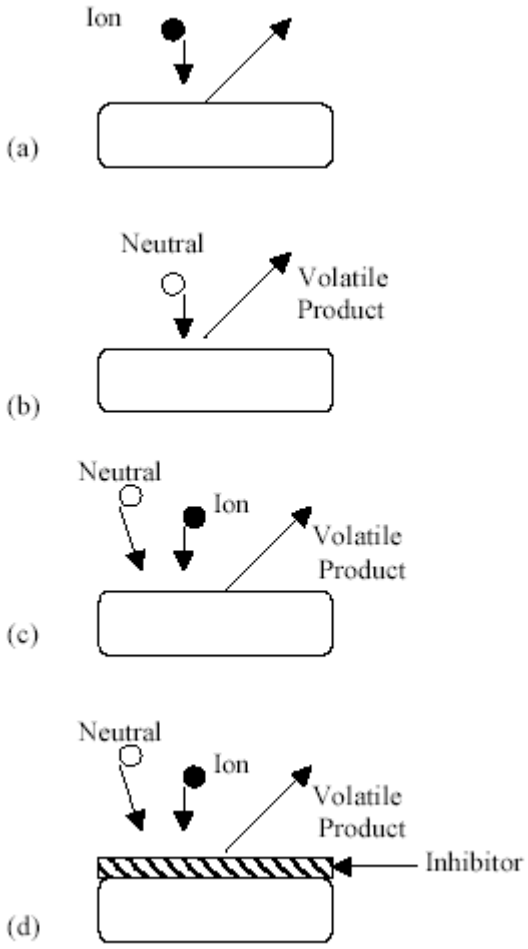

Figure 2: Plasma Etching Processes: (a) Sputtering, (b) Chemical Etching, (c) Reactive Ion Etching, and (d) Ion Inhibitor Etching.

Two main factors play a role in the amount of etching that occurs at the surface: the gas used and the flow rate. A seed gas is commonly used; helium in this study because

helium allows for breakdown and plasma generation at atmospheric pressure. When the discharge is established with helium plasma, dissociation of other atoms and/or molecules will be induced and thus the degree of etching will change, wither increasing or decreasing depending on the nature of dissociated atoms/molecules. The additions of other gas species, for example oxygen in this work, increase the etching effect because oxygen addition allows for reactive oxygen species (excited molecules, atoms, and ions) to induce etching and surface ablation. The flow rate of added etchant gases, up to a maximum point, can dramatically increase the etching rate.

2.2 Cell Adhesion

Cell behavior is influenced by the material surface properties and cell adhesion to surfaces is crucial because it precedes other cellular events, such as spreading and migration [4]. Cell adhesion is mediated by both specific and non-specific interactions. Non-specific interactions include electrostatic and van der walls forces while specific interactions predominately involve receptor-ligand binding [5]. The most important of the adhesion receptors are the integrins. These are cell surface molecules that mediate both cell-cell interactions and attachment to specific matrix proteins. Integrins are a large family of cell surface adhesive receptors, which, in the epidermis, are normally confined to the basal layer. In addition to mediating adhesion to the underlying basement membrane, integrins play a role in regulating the initiation of terminal differentiation in cell-cell adhesion and in cell migration [6]. Cadherins are another major cell adhesion molecule family responsible for calcium dependent cell-cell adhesion. Virtually all vertebrate cells seem to express one or more cadherins, according to the cell type. Some classical cadherins include E-cadherin

present in epithelia, N-cadherin located in neurons, muscle, fibroblasts, and P-cadherins on cells in the epidermis [7].

Components of the extracellular matrix also play a major role in governing cell adhesion. The extracellular matrix (ECM) includes all secreted molecules that are immobilized outside cells [8]. Two main classes of extracellular macromolecules make up the matrix: polysaccharide chains of the class called glycosaminoglycans or GAGs, and fibrous proteins including collagen, elastin, fibronectin and laminin. GAGs are usually found covalently linked to protein in the form of proteoglycans. Some proteoglycans are secreted components of the extracellular matrix and others act as co-receptors that collaborate with conventional cell-surface receptor proteins. Both bind the cells to the extracellular matrix and initiate the response of cells to some extracellular signal proteins. Cell surface receptor proteins are either ion-channel linked, G-protein linked, or enzyme linked. Collagens are the major proteins of the ECM that help support the cell. Elastin gives tissues their elasticity while fibronectin is an extracellular protein that helps cells attach to the matrix [7].

2.3 Previous Studies

The ability to control cell adhesion to synthetic polymers so that the materials support and stimulate tissue integration and reconstruction or cellular colonization is very important. It has been found that cell behavior on polymers is primarily influenced by the surface energy of the substrata [9-10]. In general, high-energy surfaces promote greater cell adhesion than low energy surfaces [11]. Synthetic polymers are often unsuitable to cell adhesion due to their low-energy surfaces, therefore requiring surface modification for the binding of specific cell molecules. The use of plasma discharge on synthetic polymers is an

excellent method for modifying the surface to make it more attractive to cells. Plasma surface modification can improve both the biocompatibility and biofunctionality of the biomaterial surface [12]. Also, exposure to plasma modifies the chemical and topographical nature of the surface of the material while keeping the bulk properties unaltered. It has previously been found that nanoscale roughness, which can be caused by plasma surface modification, contributes moderately to cell adhesion and proliferation [13]. Some researchers have shown the effects of surface wettability and plasma treated surfaces on specific cell types and will be discussed below.

The activity of keratinocytes and their progression through the cell cycle is determined by three main factors: the degree of cell differentiation, adhesion to the matrix, and the balance between growth factors and growth inhibitors [14]. In order for biomedical engineered artificial tissue to be effective, the growth factors and growth inhibitors must coincide with the synthetic material comparably to that of the human epidermis. Keratinocytes are a type of epithelial cell that express the characteristic intermediate filament proteins cytokeratins and other skin-specific proteins to form a protective barrier [6]. Keratinocyte behavior on plasma-polymerized surfaces has been investigated, however, the cells have, to date, not been seeded directly on a plasma modified polymer [15-17]. Researchers have, however, investigated epithelial cell behavior on plasma modified surfaces. Dewez [11] found that when extra cellular matrix proteins were supplied by the cells, no difference is observed between substrata that were made less hydrophobic. The extra cellular matrix proteins (collagen, laminin, fibronectin) are the primary factors that determine epithelial adhesion and migration. Jansen [10] seeded rat epithelial cells on various substrates of polystyrene dishes and measured the cell growth and attachment. Jansen

found no significant influence of surface treatment on the behavior of the epithelial cells. Xie and researchers made similar findings to Jansen in that nanoscale modification of PET by oxygen plasma discharge yielded minimal changes in epithelial cell behavior [13].

The role of surface wettability on hepatocytes has not been studied as intensely as some other cell types. Hepatocytes need attachment to the extra cellular matrix or to themselves [18-19], which suggests that the success of hepatocyte attachment strictly depends on the surface properties of the substrata. One research group examined hepatocyte adhesive functions and interactions on both hydrophobic and hydrophilic surfaces [20]. Clean glass was used as a model for hydrophilic surface and octadecylsylane-coated glass was used for a hydrophobic surface. A hepatoblastoma cell line was cultured on the substrata and adhesive interactions were characterized by the overall cell morphology, the formation of focal adhesions, and actin filaments. The cells cultured on hydrophilic glass remained single and spread well, whereas those cultured on the hydrophobic glass formed aggregates. Hepatocytes also developed pronounced actin stress fibers and focal adhesion contacts on hydrophilic glass. Hence, the hepatocyte attachment, morphology, and growth depended on the wettability of the substrata and increase with increasing hydrophilicity. Other groups have examined the effect of using a plasma modified surface for specific binding of biomacromolecules to promote hepatocyte adhesion [21]; however, they have not studied the direct effects of plasma-modified surface and primary hepatocyte culture.

To date, no literature exists that determines the effects of keratinocyte and hepatocyte growth, proliferation, and adhesion to plasma treated PET. Therefore, this work examines these effects to gain a better understanding of how surface chemistry and surface topography influences cell behavior.

III. EXPERIMENTAL

3.1 Materials

Polyethylene terephthalate (PET) film was purchased from McMaster-Carr (product number 8567K52). The film is made from ethylene glycol and dimethyl terephthalate and it is a thermoplastic film comparable to Mylar®. The PET had a tensile strength of 28,000 psa and a coefficient of thermal expansion of 23 x 10^{-5} in./in./°C.

The keratinocytes were supplied by the laboratory of Dr. Nancy Monteiro-Riviere at the Veterinary School at North Carolina State University. The keratinocytes were freshly isolated from the dorsal area of a pig and were cryogenically stored until used [22]. The cells were cultured in Keratinocyte Basal Media (Cambrex) supplemented with 1% fetal bovine serum, bovine pituitary extract, human epidermal growth factor, insulin, hydrocortisone, gentamicin, epinephrine, and transferrin supplied by the manufacturer.

The hepatocytes were supplied by Dr. David Gerber's laboratory at the University of North Carolina at Chapel Hill. The hepatocytes were freshly isolated from C57Bl/6 mice using a modification of the two stage liver perfusion technique described by Seglen [23-24]. The hepatocytes were cultured in Dulbecco's Modified Eagle's Media (DMEM - Sigma) containing 10% Fetal Bovine Serum, hepes, nicotinamide, L-proline, L-ascorbic acid 2-phosphate, dexamethasone, antimycotic-antifungal, and insulin-transferrin-selenium.

The fluorescent probe used to stain the cells was purchased from Molecular probes (product number C1157). This product is a fluorescein-based tracer for very long-term cell labeling. The probe permeates the cell membrane and once inside, is cleaved off by non-

specific esterases, resulting in a charged form that leaks out of the cell far more slowly than its parent compound.

3.2 Plasma Treatment

3.2.1 Atmospheric Plasma Facility

The atmospheric plasma facility, located at North Carolina State University in the College of Textiles, is a capacitively-coupled dielectric barrier discharge (DBD) operated by a 4.8 kW audio frequency power supply at 4-10 kHz [25]. Two transformers 180^{o} out of phase coupled to the power supply provide the high voltage to the electrodes. The device has an active exposure area of approximately 60 x 60 cm between two copper electrodes with 5 cm gap separation. Helium gas is used to initiate the discharge and is injected between the electrodes into the test cell at a constant flow rate of approximately 10L/m. Depending on the desired treatment, other gases such as oxygen, argon, nitrogen, hydrogen, CF_4, C_3F_6, CH_4, and CO_2 could be added at a specific flow rate into the test cell. The dielectric-barrier discharge is a non-equilibrium discharge generates low-temperature (1-2eV), low electron number density (10^{14} - 10^{16} /m^3) pseudo-glow discharge plasma which is typical for dielectric-barrier discharges at atmospheric pressure [26-28]. Electron-neutral collision is dominant as the ionization fraction is low, and thus the plasma conductivity is determined by both electron-neutral and electron-ion collisions with much less contribution from electron-ion collisions [29]. The discharge generates electrons, ions, excited atoms and molecules, as well as UV radiation. Careful addition of other gases into the helium flow prevents development of streamers and makes the discharge very uniform between the two electrodes inside the treatment active volume [28-29].

The device is capable of batch treatment of films and fabric pieces using a test cell, as well as continuous operation using the roller feed system for large fabric rolls or continuous filaments and yarns. Figure 3 shows a schematic drawing of the device in which the substrate represents batch treatment inside the test cell and the roller system represents continuous treatment of fabrics and yarns.

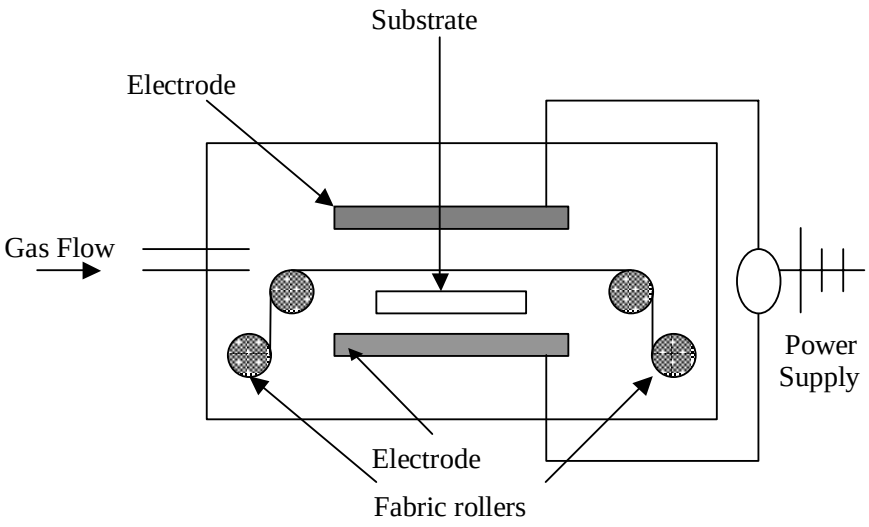

Figure 3: Schematic Drawing of the Atmospheric Plasma Device

Figure 4 shows a simplified circuit diagram of the device, in which C_T and R are coupling capacitors and resistors, and C represents the two electrodes in the capacitively-coupled mode. The step-up transformers are at 180^o out of phase, and the HVP are the locations of HV probes for voltage measurements.

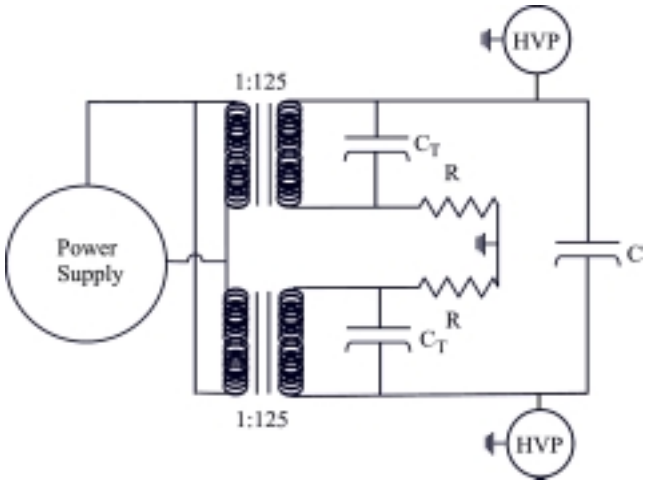

Figure 4: Schematic Circuit Diagram of the Atmospheric Plasma DBD Device

In this study all samples were exposed to plasma using the test cell. Input power, operating voltage, frequency and plate separation were all held constant. The helium gas flow rate was held at approximately 10 L/m and other gas mixes, oxygen or CF4, were added at 1% into the flow stream. In order to achieve proper gas mixtures when plasma treating, the plasma device uses a four-channel mass flow controller to power and monitor the flow rate. The flow rate for a mass controller is determined by the magnitude of the set point signal and is calculated using the equation (Eq. 1) below:

Corrected Flow Rate (CFR) = *Set Point Signal* × *Gas Correction Factor (GCF)* **Eq. 1**

The gas correction factor is used to indicate the ratio of flow rates of different gases which will produce the same output voltage from a mass controller. This is a function of the specific heat, density, and molecular structure of the gases that are to be used. Nitrogen is used as the baseline gas (GCF = 1) since the flow controllers are calibrated with nitrogen. The equations are shown below:

For pure gases:

$$GCF_x = \frac{0.3106 \times S}{dx\ Cp_x} \qquad \textbf{Eq. 2}$$

where:

GCF_x = Gas correction factor for gas X

0.3106 = (Standard density of nitrogen) (Specific Heat of nitrogen)

S = Molecular Structure correction factor where S equals

1.030 for Monatomic gases

1.000 for Diatomic gases

0.941 for Triatomic gases

0.880 for Polyatomic gases

d_x = Standard Density of gas X, in g/l (at 0ºC and 760 mm Hg)

cp_x = Specific Heat of gas X, in cal/gºC

For Helium:

$$GCF_{He} = \frac{0.3106 \times 1.0}{0.1786 \times 1.241} = 1.4$$

For Oxygen:

$$GCF_{O_2} = \frac{0.3106 \times 1.0}{1.427 \times 0.2193} = 0.993$$

For A Mixture of Two Gases:

$$GCF_{Mix} = \frac{0.3106 \times (a_1 S_1 + a_2 S_2)}{a_1 d_1 Cp_1 + a_2 d_2 Cp_2} \qquad \textbf{Eq. 3}$$

where:

GCF_{Mix} = Gas correction factor for gas X

0.3107 = (Standard density of nitrogen) (Specific Heat of nitrogen)

a_1 and a_2 = Fractional flow of gases 1 and 2 (a_1 and a_2 must add up to 1)

S_1 and S_2 = Molecular Structure correction factor for gases 1 and 2 where s equals:

1.030 for Monatomic gases

1.000 for Diatomic gases

0.941 for Triatomic gases

0.880 for Polyatomic gases

d_1 and d_2 = Standard Density of gases 1 and 2, in g/l (at 0ºC and 760 mm Hg)

Cp_1 and Cp_2 = Specific Heat of gas 1 and 2, in cal/gºC

For a mixture using 99% helium and 1% oxygen, the gas correction factor would be:

$$GCF_{He-O_2} = \frac{0.3106\times(0.99\times1+0.01\times1)}{0.99\times0.1786\times1.241) + 0.01\times1.427\times0.2193} = 1.396$$

Using the above equations and the flow for helium set to 10 L/min, the set point signals for 99% helium and 1% oxygen plasma is 10 L/min and 0.14 L/min, respectively. This calculation is shown below:

$$CFR_{He} = 10.00\ L/\min \times 1.40 = 14.00$$

For a 99% helium and 1% oxygen plasma:

$$0.01 = \frac{(X)\times(0.993)}{14.00}$$

From which the set point for Oxygen = 0.14 L/min

For this study, the PET films were cut into 4 x 6 inch sheets and soaked in 70% ethanol for 5 minutes. The films were taken out of the ethanol bath and further rinsed with 70% ethanol. The films were then divided among seven treatment groups: untreated (control), helium plasma for 30 seconds, helium plasma for 60 seconds, helium plasma for 90 seconds, helium/oxygen plasma for 30 seconds, helium/oxygen plasma for 60 seconds, and helium/oxygen plasma for 90 seconds (Table 1). Each group was then treated accordingly in the plasma chamber with the settings as stated above. After treatment in the plasma chamber, the films were placed in a labeled storage bag. One sample of each of the treatment groups was further divided into seven experiments: films stored at ambient temperature used for contact angle testing, films stored at ambient temperature used for atomic force microscopy studies, films stored at 0°F for contact angle testing, films stored in keratinocyte media at 37°C for contact angle testing, films stored in hepatocyte media at 37°C for contact angle testing, films stored at room temperature for antistatic testing, and films stored at room temperature used for plating cells.

Treatment Type	Code used Throughout Paper
Non-plasma treated PET	Untreated PET
Helium plasma treated PET for 30 seconds	He 30
Helium plasma treated PET for 60 seconds	He 60
Helium plasma treated PET for 90 seconds	He 90
Helium/Oxygen plasma treated PET for 30 seconds	He/O 30
Helium/Oxygen plasma treated PET for 60 seconds	He/O 60
Helium/Oxygen plasma treated PET for 90 seconds	He/O 90

Table 1: Nomenclature for plasma treatments.

3.2.2 Contact Angle

The hydrophobicity/hydrophilicity of the PET films stored at ambient temperature, 0°C, in keratinocyte media at 37°C, and in hepatocyte media at 37°C was quantified by the sessile droplet method [30-31]. This test was conducted in accordance with the ASTM method D5946-04 (Standard Test Method for Corona-Treated Polymer Films Using Water Contact Angle Measurements) using a goniometer [32]. The advancing and receding angles of the deionized water droplet formed on the polymer surface were recorded and repeated three times. This test was performed 15 minutes after plasma treatment and every day for ten days. The average contact angle was calculated and graphed in correlation to day post treatment.

3.2.3 Antistatic Tests

The presence of electrical charges on a surface has been shown to play a role in determining cell behavior [11]. Because of this phenomenon, the antistatic property of the plasma treated PET was analyzed. Static charging of polymer surfaces can be caused by the presence of loosely bound ions from the air or a discharging process in which ions are supplied to neutralize existing charges [33]. This charge can be measured by its rate of decay and the sign, whether it is positive or negative [34]. Non-destructive static decay was conducted using Electro-tech systems Model 806A test fixture with ETS Model 406 static decay meter inside a Model 518 automatically controlled environmental chamber. The untreated and plasma treated PET samples were charged to 5kV with both positive and negative polarity tests and with a cutoff rate at 50%. The maximum decay time was 90 seconds and each sample test was repeated three times to ensure accurate results.

3.2.4 Atomic Force Microscopy

A JOEL JSMP 5200 Environmental Scanning Probes Microscope was used to analyze the film surfaces. Intermittent tapping mode was used to scan the surface at a spring constant of 40 kHz and resonant frequency of 300 kHz. Two areas of each film were scanned, one at 1 μm^2 and the other at 5 μm^2. The films were analyzed immediately after plasma treatment as well as two days and five days post treatment. The average surface roughness and root mean square roughness was then calculated for each sample and area scanned.

3.3 Cell Studies

3.3.1 Keratinocytes

The cryopreserved keratinocytes were warmed in a 37°C water bath until thawed. The viability and cell concentration of the keratinocytes was determined using a hemacytometer. A hemacytometer, or counting chamber, is a glass slide with a grid containing nine larger squares that are 1 mm^2 in area (Figure 5). A glass cover slip is placed on top of the hemacytometer so that distance between the hemacytometer and cover slip is precisely 0.1 mm (Figure 6). The viability of the cells is determined using a dye exclusion test where the dead cells take up the dye, normally trypan blue, because their membranes are not intact.

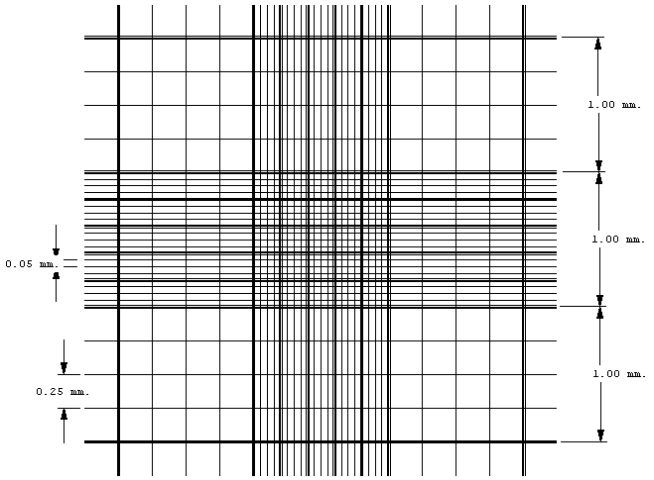

Figure 5: Dimensions of a Typical Hemacytometer.

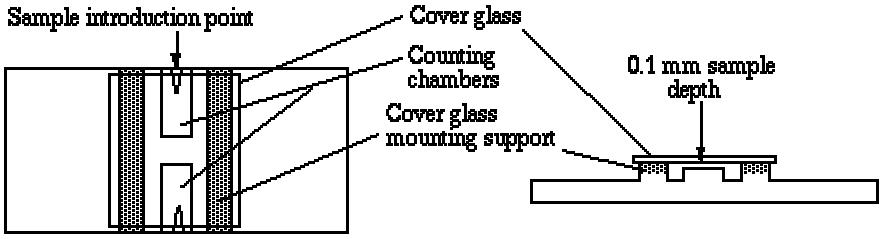

Figure 6: Diagram of a Hemacytometer and Cover Slip.

A solution of 80 µL DMEM, 10 µL of trypan blue, and 10 µL of the cell suspension was prepared and added to a tube. After one minute, 10 µL of the solution was applied to the hemacytometer and the number of live and dead cells were counted. The concentration of cells per milliliter and viability were determined using the following formulas:

$$Cell\ concentration\ per\ mL\ = \frac{Total\ number\ of\ cells\ counted\ \times\ dilution\ factor\ \times 10^4}{Number\ of\ squares\ counted}$$

Eq. 4

$$Viability = \frac{Number\ of\ cells\ unstained \times 100}{Total\ number\ of\ cells} \quad \textbf{Eq. 5}$$

The amount of cells needed was pipetted into a 15 mL conical tube with 5 mL of fresh keratinocyte media in it. The cell mixture was centrifuged at 100 x gravity for three minutes. The supernatant was aspirated off and the cells were brought up in keratinocyte media. The keratinocytes were seeded at a density of 80,000 cells per well.

3.3.2 Hepatocytes

The freshly isolated hepatocytes were received in a 50 mL conical tube with the viability and cell number previously determined. The cells were centrifuged at 100 x gravity for three minutes. The supernatant was aspirated off and the cells were brought up in hepatocyte media. The hepatocytes were seeded at a density of 62,500 cells per well.

3.3.3 Plating Method

Cells were plated immediately following plasma treatment (Day 0), two days after plasma treatment (Day 2), and five days after plasma treatment (Day 5). The procedure described herein was performed three times: day 0, 2, and 5. The outside of the storage bags containing the plasma treated PET films were sprayed with 70% ethanol and placed inside a laminar flow hood. Using a specialized hole puncher, 8 rounds of each plasma treated film and 16 rounds of untreated film were punched. Each type of treated round was placed in a labeled 60 mm^2 dish. 70% ethanol was added to the dish and the films were swirled in the ethanol bath. The films were taken out of the dish and dried on a Kimwipe from inside the hood. Five sets of four 24-well plates were labeled “HA”, “HB”, “KA”, “KB” which stand

for hepatocyte plate A, hepatocyte plate B, keratinocyte plate A, and keratinocyte plate B, respectively. The plates used were non-tissue-culture-treated polystyrene. Using the wooden end of a sterile cotton tip applicator, a dab of silicone type A glue was added to the middle of each well in one column of the plate. According to the layout in Figure 7, the appropriate film was then added to the four wells in the column. This step was repeated for each remaining column.

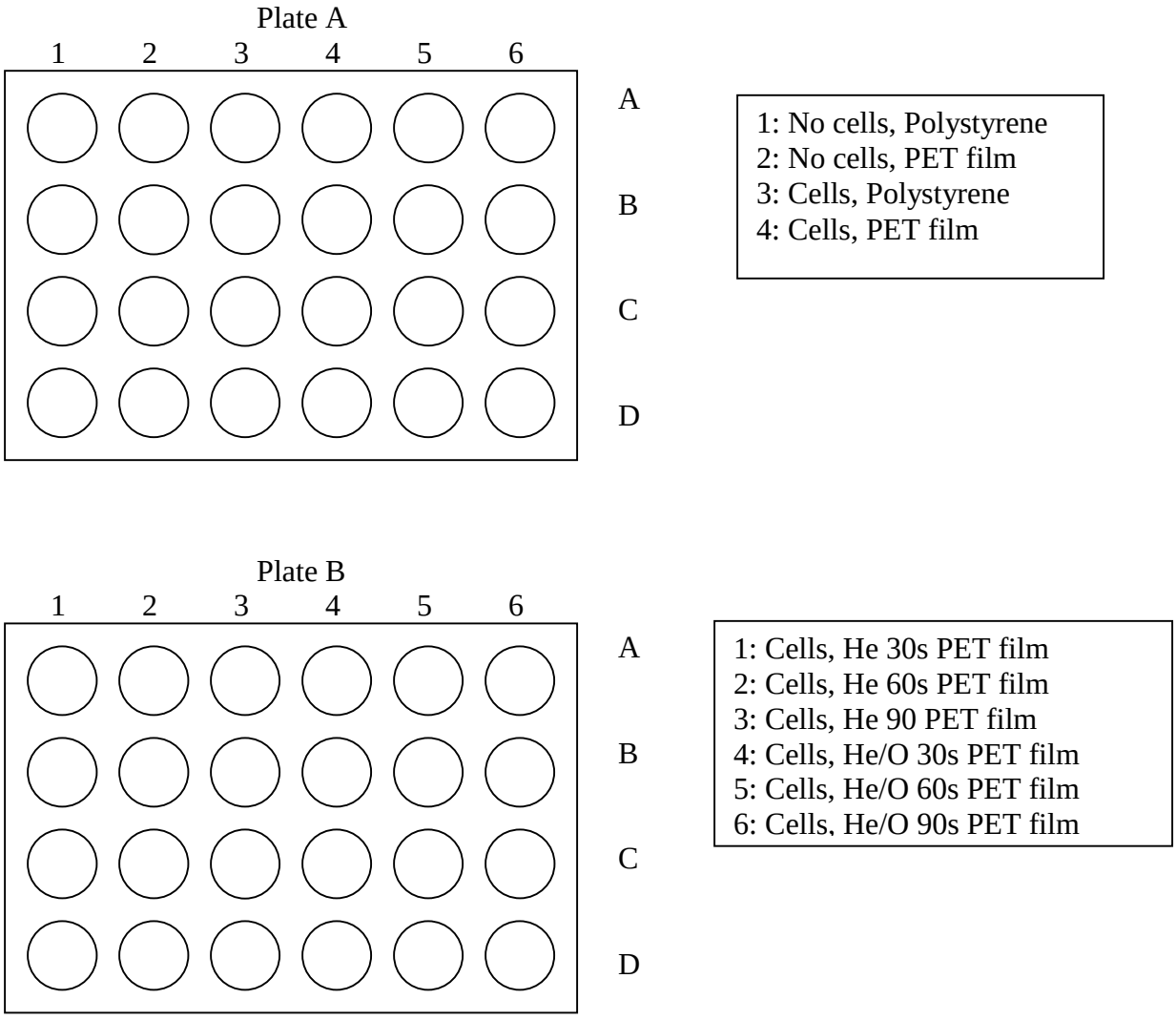

Figure 7: Plate Design

When all of the films were secured in the wells, 300 µL of phosphate buffered saline (PBS) was added to each well. The plate was swirled several times to ensure all of the liquid covered the well surface and then it was aspirated off. The media or cells in media were then added to the appropriate wells. The plates were then placed in a humidified incubator at 37°C and 5% CO_2. The media was changed one day and four days after plating by aspirating the existing media and replacing it with fresh warmed media.

3.3.4 Proliferation and Adhesion Method

The proliferation and adhesion tests were run at 12 hours, 24 hours, 48 hours, 72 hours, and 144 hours after plating or Day 0.5, 1, 2, 3, and 6. Figure 8 shows an overview of the schedule for the experiments. Words in red stand for cells plated at Day 0, words in blue stand for cells plated at Day 2, and words in green stand for cells plated at Day 5. The black words are non cell related experiments.

Day 0 Plasma protocol Contact Angle AFM Antistatic Plate Cells	**Day 0.5** Test cells	**Day 1** Contact angle Test cells Change media	**Day 2** Contact angle AFM Antistatic Test cells Plate cells	**Day 2.5** Test cells
Day 3 Contact angle Test cells Test cells Change media	**Day 4** Contact angle Change media Test cells	**Day 5** Contact angle AFM Antistatic Test cells Plate cells	**Day 5.5** Test cells	**Day 6** Contact angle Test cells Change media Test cells Change media
Day 7 Contact angle Test cells	**Day 8** Contact angle Test cells Test cells	**Day 9** Contact angle Change media	**Day 10** Contact angle	**Day 11** Contact angle Test cells

Figure 8: Schedule of Experiments

To perform the proliferation and adhesion assay, the fluorescent dye must first be prepared. 500 µg of the probe was dissolved in 90 µL of DMSO – this resulted in a 10 mM concentration. 1.5 µL of the 10 mM stock solution was dissolved in 10 mL of PBS to yield a final working concentration of 1.5 µM. The PBS solution containing the probe was warmed in the 37°C water bath and then placed in a laminar flow hood. The existing media was aspirated from the culture wells and 350 µL of the pre-warmed solution was added in each well. The plates were incubated for 15 minutes at 37°C and 5% CO_2. The wells were then washed with 500 µL of fresh pre-warmed media (either keratinocyte or hepatocyte media depending on the cell type) and 500 µL of media was added to each well. The plates were again incubated for 1 hour. The fluorescence value of each well at 540 nm was then read

using a GENios plate reader by Tecan and recorded. The plates were then placed on a bench and the cover was removed. Approximately 3.5 mL of PBS was added to each well so that a positive meniscus formed. Adhesive film specifically made for PCR application was placed over each plate. The film was secured to the plates using a rubber roller. In order for the cells to remain in a homogeneous medium, there were no bubbles trapped in the wells underneath the adhesive film. The plates were then inverted and placed in a plate holder in a centrifuge. The plates were centrifuged at 1000 rpm for 5 minutes. When the plates were finished centrifuging, they were carefully taken out of the centrifuge and placed right side up. The film was removed and all of the contents of the plate were emptied in a trash can to remove all of the liquid in the wells. 500 µL of fresh media was added to each well and the fluorescence was measured using a GENios plate reader. These values were recorded as "after centrifuge." The background was subtracted from each fluorescent value before the proliferation and adhesion were quantified.

To calculate the proliferation, the following formula (Eq. 6) was used. The value at day 0.5 was used as the reference value.

$$Proliferation = \frac{Fluorescence\ at\ Time\ X\ -\ Fluorescence\ at\ Time\ 0.5}{Fluorescence\ at\ time\ X} \times 100 \quad \textbf{Eq. 6}$$

To calculate the adhesion, a similar formula (Eq. 7) to the one above was used:

$$Percent\ of\ Cells\ Lost\ = \frac{Final\ -\ Initial}{Initial} \times 100 \quad \textbf{Eq. 7}$$

3.4 Statistical Analysis

Multiple analysis of variance (MANOVA) was performed on the data using Statistical Analysis Software (SAS Institute, Inc., version 9.1.3). MANOVA was used to determine the effects of day plated, day tested, and gas used in the plasma on the growth and adhesion of keratinocytes and hepatocytes. Throughout the statistical analysis, a probability of less than 0.05 was considered a significant effect.

IV. RESULTS AND DISCUSSION

4.1 Contact Angle Measurements

After the PET films were plasma treated, they were stored in air, the freezer, keratinocyte media, or hepatocyte media for ten days. The contact angle was measured once each day and the results are shown in Figures 9-12 and tabulated in the Appendix. Plasma treatment of the PET films dramatically changed the surface chemistry. For all treatment types, the contact angle decreased, and thus the surface became much more hydrophilic. When the films were stored in air at room temperature (Figure 9), the hydrophilicity decreased until day five where a plateau was then reached. The surface chemistry never reverted back to the original contact angle, however it did increase much more than the films stored in the freezer (Figure 10). With just 15 minutes of storage in the freezer, the films had a lower contact angle than those stored at room temperature. The contact angle remained at the lower values for the entire ten days, never going above 63°. This demonstrates that the temperature influences the rate that the surface regresses to near original hydrophobicity and helps to preserve the effects of the plasma discharge treatment.

The effect of the plasma treated films soaked in keratinocyte media and hepatocyte media on the contact angle are much different than the films stored in air at room temperature (Figures 11 and 12). For both media types, the surface became more hydrophilic and the contact angle of the film dropped significantly during the 15 minutes to 24 hours after plasma treatment. Due to this change, a new set of films were plasma treated and the contact angle

of films in the medias were taken at 5, 10, 15, 30, 60, 120, and 180 minutes as shown in Figure 13.

The films stored in the keratinocyte media began to significantly change between 15 and 30 minutes where as the films stored in the hepatocyte media began to change between 30 and 60 minutes. This significant change is believed to be due to the presence of proteins in the media. Both media types are supplemented with fetal bovine serum (FBS) which contains high levels of proteins, however, the keratinocyte media has only 1% FBS versus the hepatocyte media which has 10% FBS. This difference in FBS may also be the reason why the PET in hepatocyte media maintains a lower contact angle than the PET in keratinocyte media throughout the ten-day trial. Müller documents that protein absorption and activity is strongly related to surface roughness on the nanometer scale. Also, small changes in surface composition such as carbon and oxygen content are inconsequential in wetting and protein absorption of surfaces [35]. The changes in surface hydrophilicity of the plasma treated PET may have a greater effect on cell behavior than was previously thought.

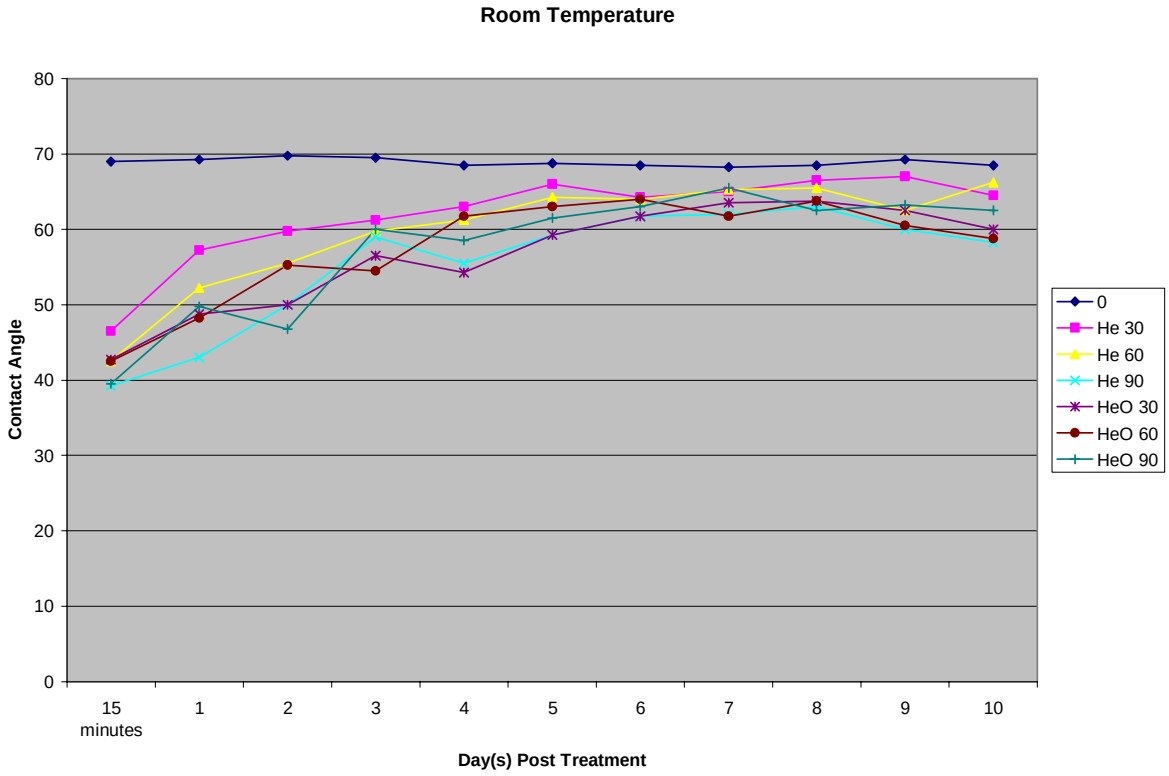

Figure 9: Contact Angle of Films Stored in Air at Room Temperature

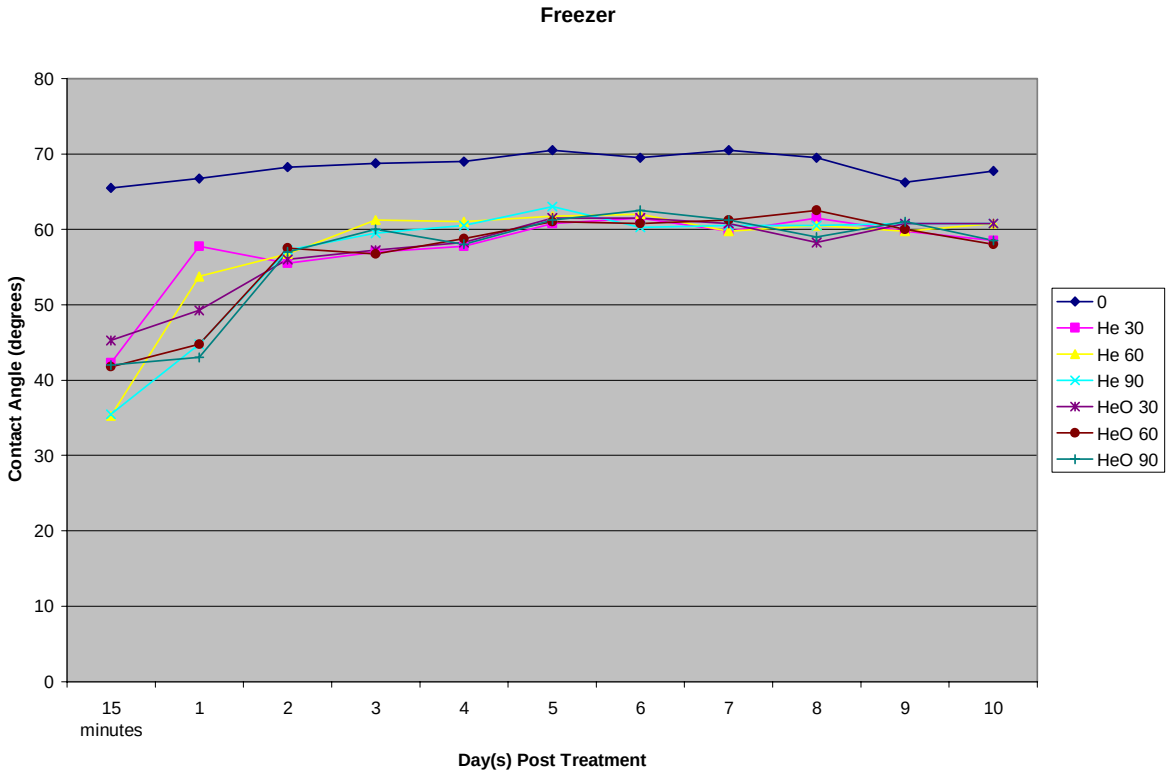

Figure 10: Contact Angle of Films Stored in a Freezer.

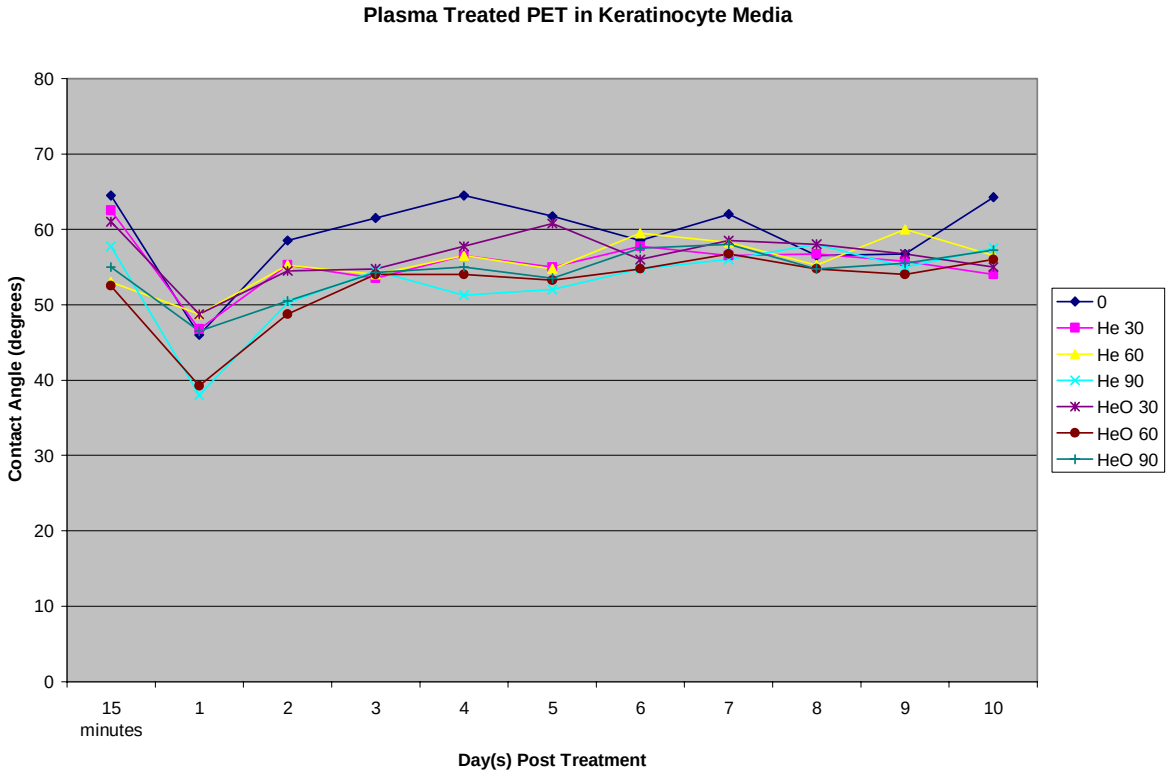

Figure 11: Contact Angle of Films Stored in Keratinocyte Media.

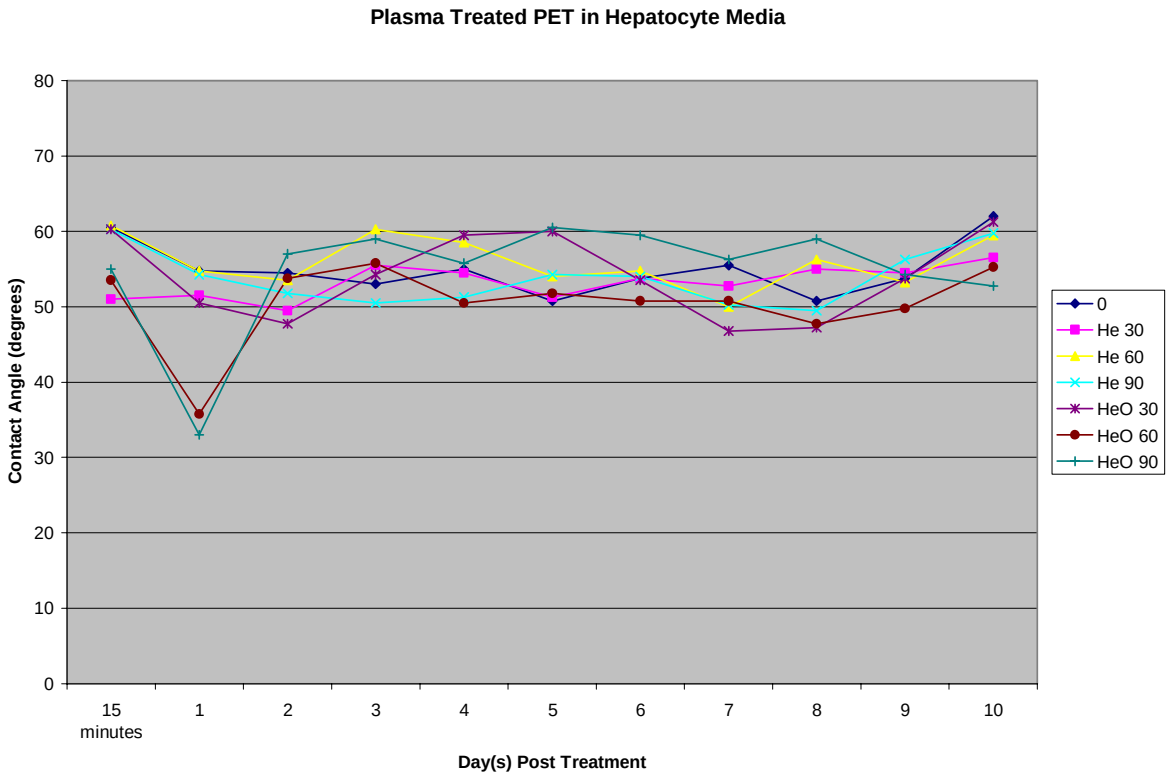

Figure 12: Contact Angle of Films Stored in Hepatocyte Media.

(a)

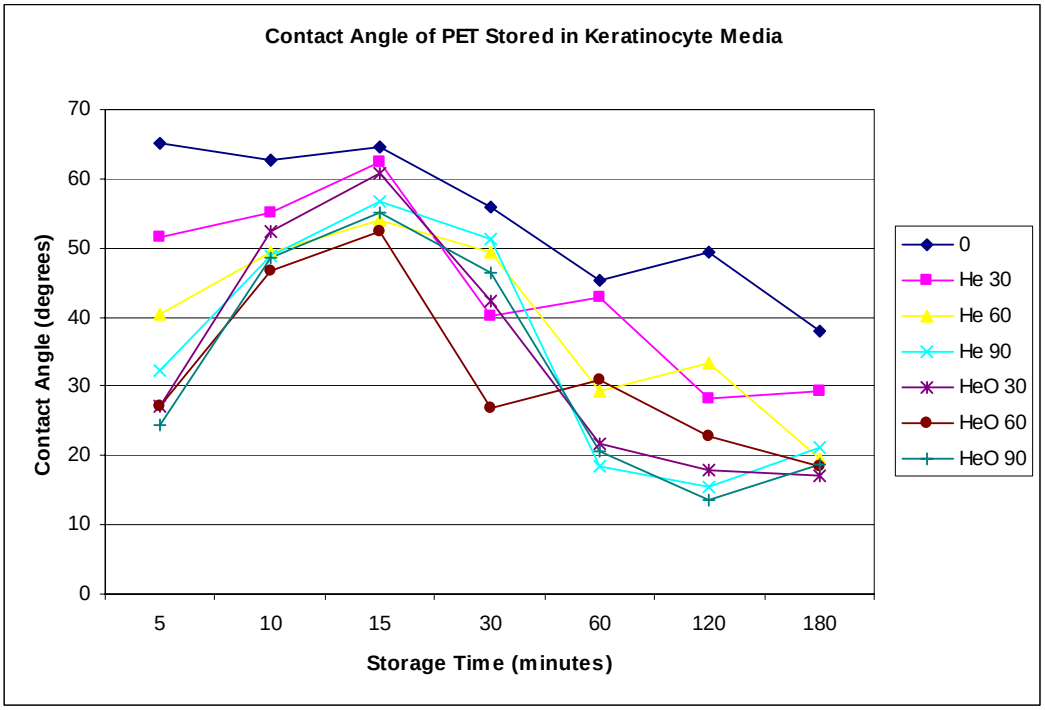

(b)

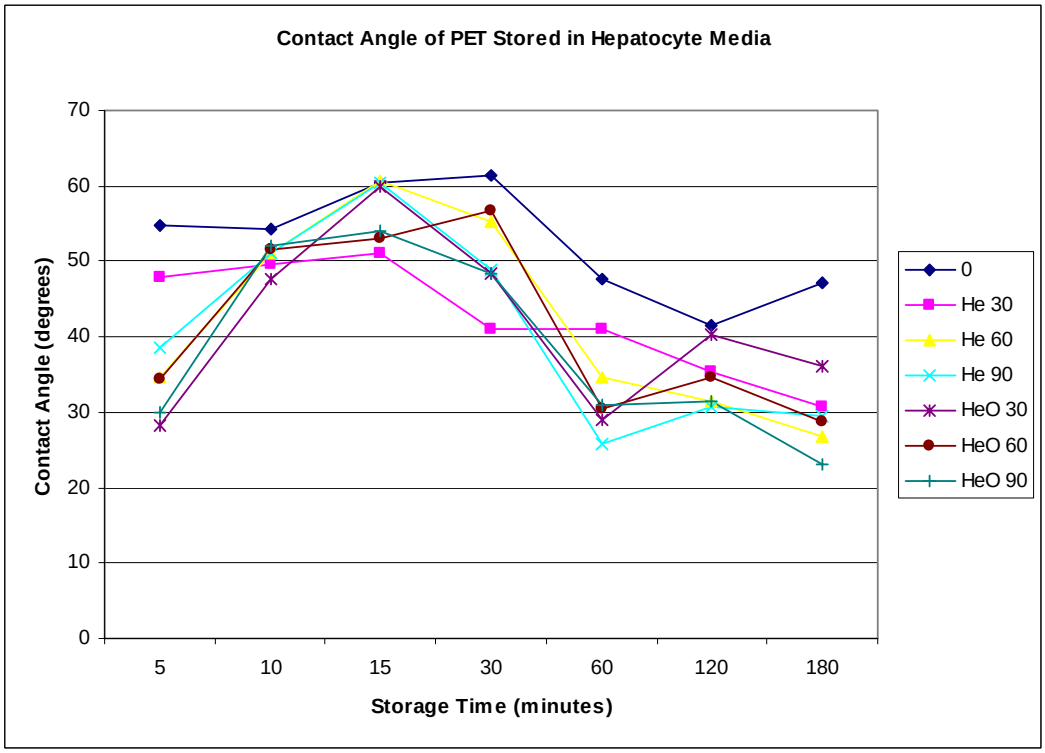

Figure 13: Short Time Span Contact angle of Plasma Treated PET films Stored in (a) Keratinocyte Media and (b) Hepatocyte Media

4.2 Antistatic Test

The antistatic test did not reveal any differences in the untreated PET films and the treated PET films. As shown in Table 5, each sample held 5 kV for the entire 90 seconds, tested at both positive and negative polarities, revealing that it is not antistatic.

		Sample						
		Control PET	He 30	He 60	He 90	He/O 30	He/O 60	He/O 90
Polarity	+	>90 sec	>90 sec	>90 sec	>90 sec	>90 sec	>90 sec	>90 sec
	+	>90 sec	>90 sec	>90 sec	>90 sec	>90 sec	>90 sec	>90 sec
	+	>90 sec	>90 sec	>90 sec	>90 sec	>90 sec	>90 sec	>90 sec
	-	>90 sec	>90 sec	>90 sec	>90 sec	>90 sec	>90 sec	>90 sec
	-	>90 sec	>90 sec	>90 sec	>90 sec	>90 sec	>90 sec	>90 sec
	-	>90 sec	>90 sec	>90 sec	>90 sec	>90 sec	>90 sec	>90 sec

Table 2: Results from the antistatic test: decay time in seconds.

The PET, both untreated and treated, is considered not antistatic because it did not repel the charges. The researcher did not want to functionalize the surface by adding antistatic properties that could interfere with cell behavior. The test determined that cell growth, proliferation, and adhesion were not governed by the static properties of the polyethylene terephthalate films.

4.3 Atomic Force Microscopy

Atomic force microscopy (AFM) was used to visualize and compare the topography of untreated and treated surfaces. AFM images are compared and, after plasma treatment, different morphological structure was observed depending on the type of the sample (Figures 14-19).

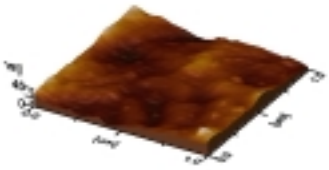

(a) No Treatment

(b) Helium 30

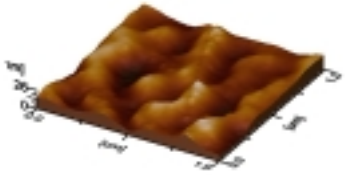

(c) Helium 60

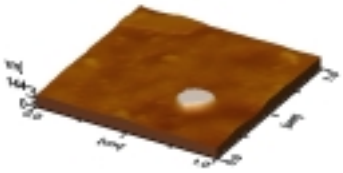

(d) Helium 90

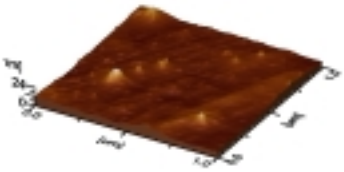

(e) Helium/Oxygen 30

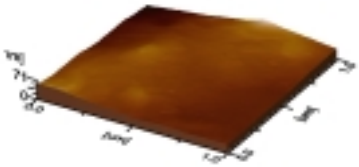

(f) Helium/Oxygen 60

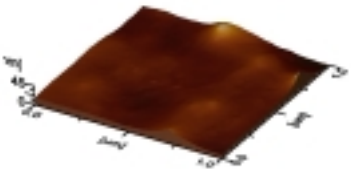

(g) Helium/Oxygen 90

Figure 14: 3D Pictures of Pet Film Imaged the Day of Treatment at 1 μm^2.

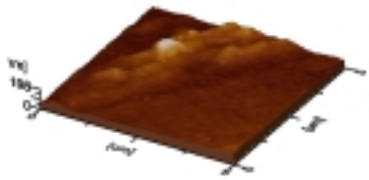

(a) No Treatment

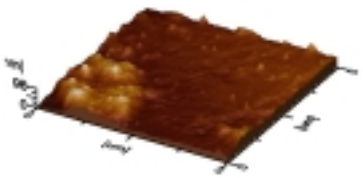

(b) Helium 30

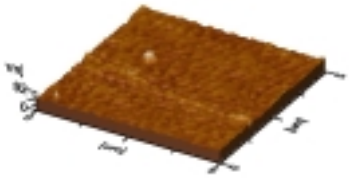

(c) Helium 60

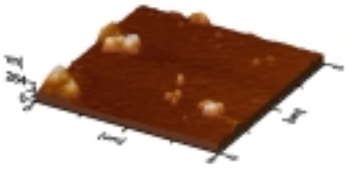

(d) Helium 90

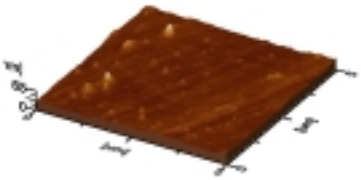

(e) Helium/Oxygen 30

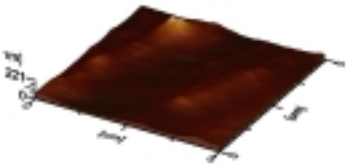

(f) Helium/Oxygen 60

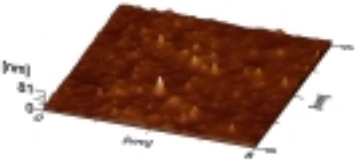

(g) Helium/Oxygen 90

Figure 15: 3D Pictures of Pet Film Imaged the Day of Treatment at 5 μm^2.

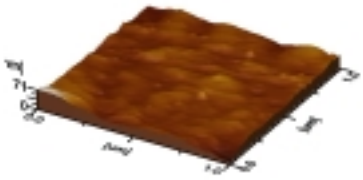

(a) No Treatment

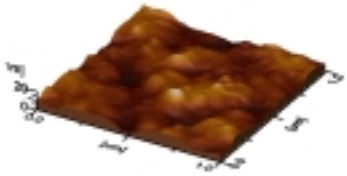

(b) Helium 30

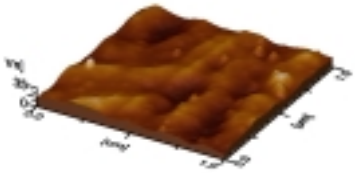

(c) Helium 60

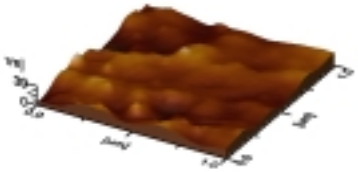

(d) Helium 90

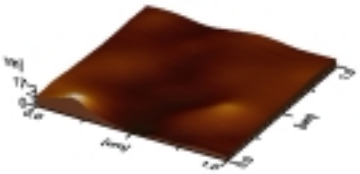

(e) Helium/Oxygen 30

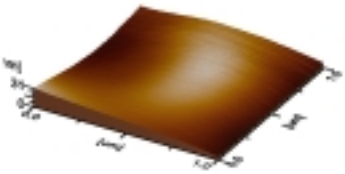

(f) Helium/Oxygen 60

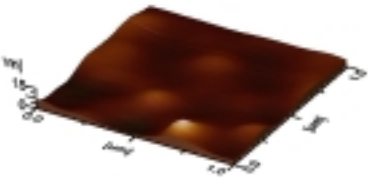

(g) Helium/Oxygen 90

Figure 16: 3D Pictures of Pet Film Imaged Two Days after Treatment at 1 μm^2.

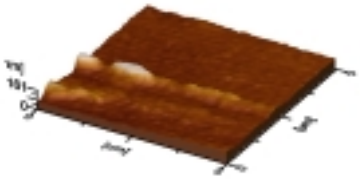

(a) No Treatment

(b) Helium 30

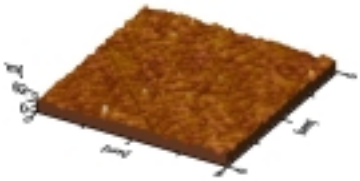

(c) Helium 60

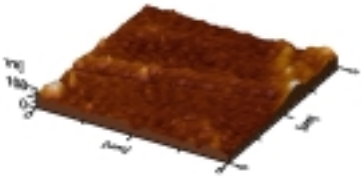

(d) Helium 90

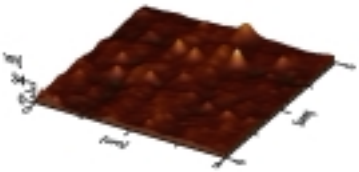

(e) Helium/Oxygen 30

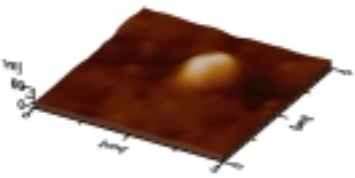

(f) Helium/Oxygen 60

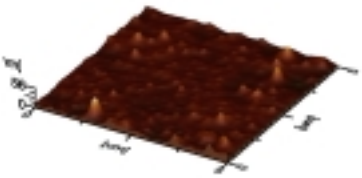

(g) Helium/Oxygen 90

Figure 17: 3D Pictures of Pet Film Imaged Two Days after Treatment at 5 μm^2.

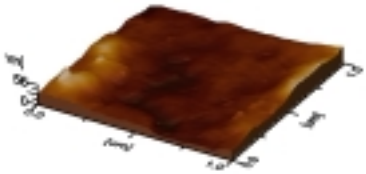

(a) No Treatment

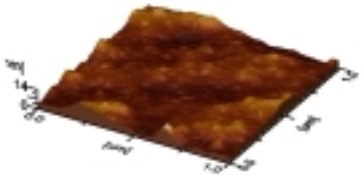

(b) Helium 30

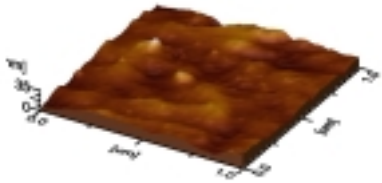

(c) Helium 60

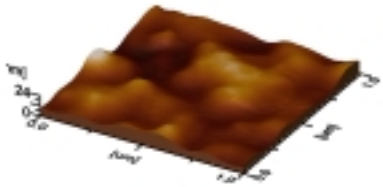

(d) Helium 90

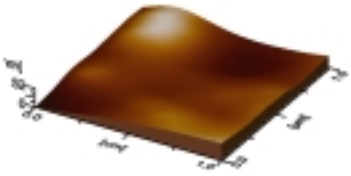

(e) Helium/Oxygen 30

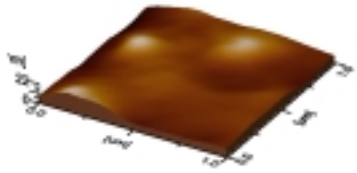

(f) Helium/Oxygen 60

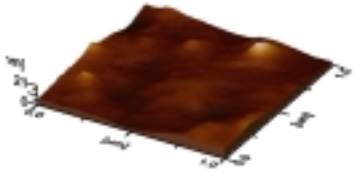

(g) Helium/Oxygen 90

Figure 18: 3D Pictures of Pet Film Imaged Five Days after Treatment at 1 μm^2.

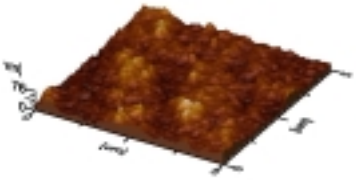

(a) No Treatment

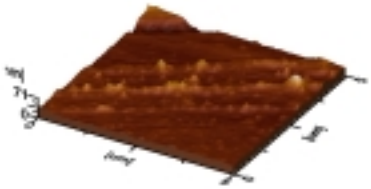

(b) Helium 30

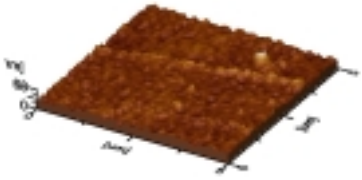

(c) Helium 60

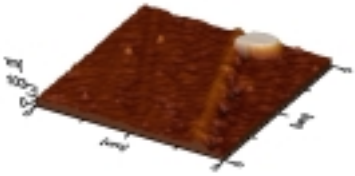

(d) Helium 90

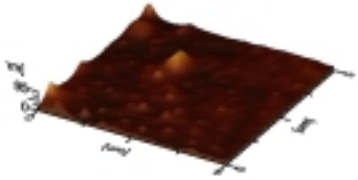

(e) Helium/Oxygen 30

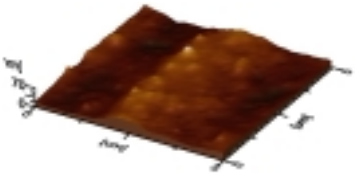

(f) Helium/Oxygen 60

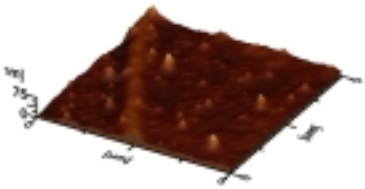

(g) Helium/Oxygen 90

Figure 19: 3D Pictures of Pet Film Imaged Five Days after Treatment at 5 μm^2.

The AFM images show helium plasma treated PET created a rougher surface when compared to the untreated PET. Also, the addition of oxygen into the plasma further increased the degree of etching, thus making the surface smoother by the removal of excess particulates residing on the surface. Plasma excited species, atoms, and ions induce surface activation of PET, thus causing surface etching, ablation, and possible scission. Including oxygen into the plasma further allows excited oxygen atoms and ions to chemically interact more with the surface. Due to possible scissions, radicals generated in the plasma discharge are redeposited on the surface or cross-linked to the fibers. The addition of oxygen (1%) into

the plasma stream helped to etch non-uniform features on the surface, thus resulting in smoother surface topography. These images of surface topography are correlated with quantitative texture parameters, such as average roughness and root mean square roughness, and are graphically presented in Figures 20 and 21, respectively and tabulated in the Appendix.

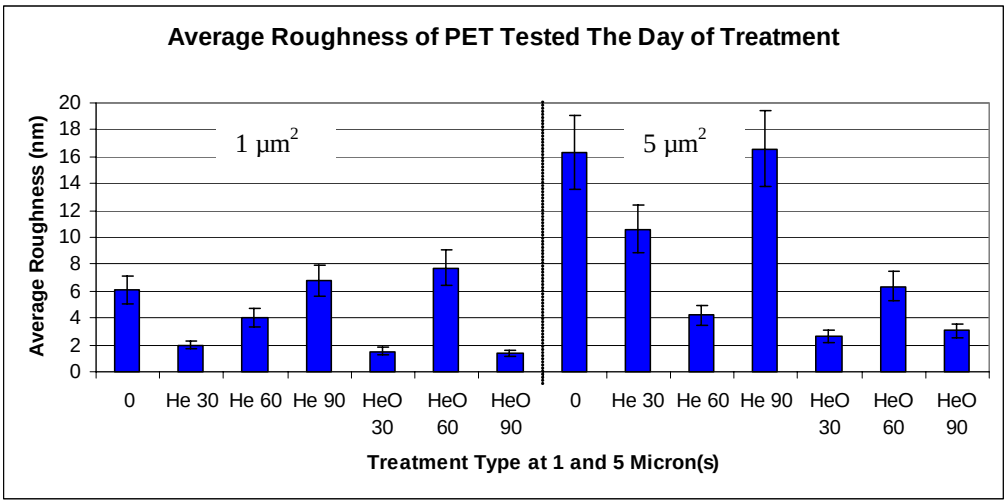

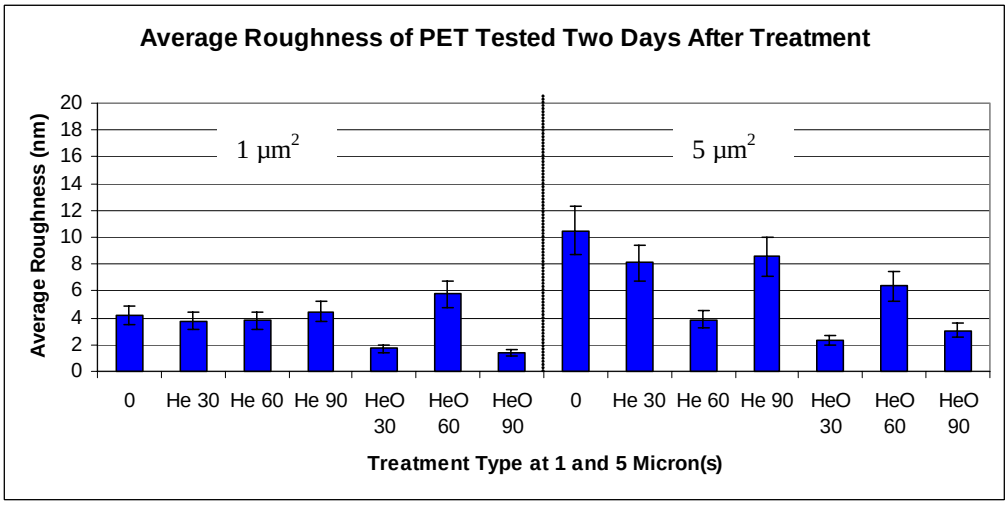

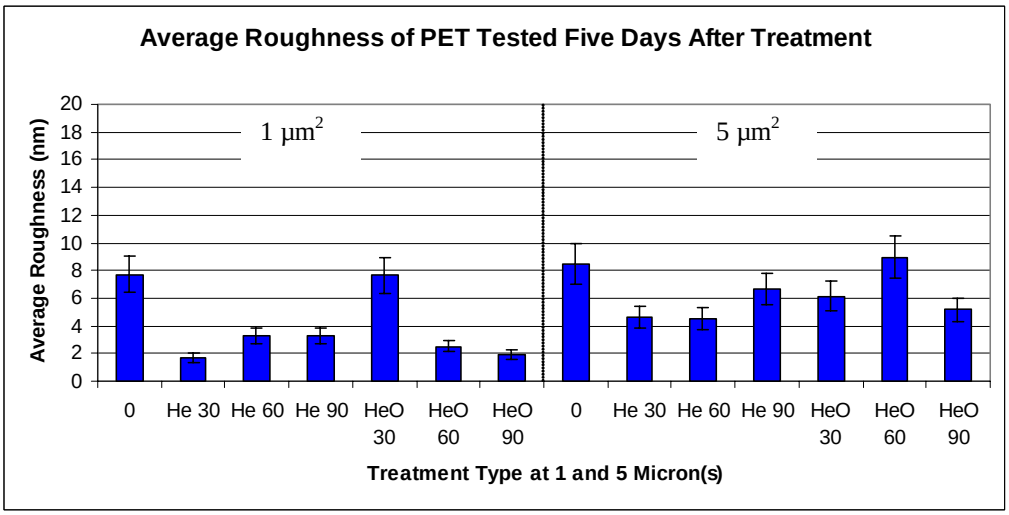

Figure 20: Graphical representation of the average roughness of PET films.

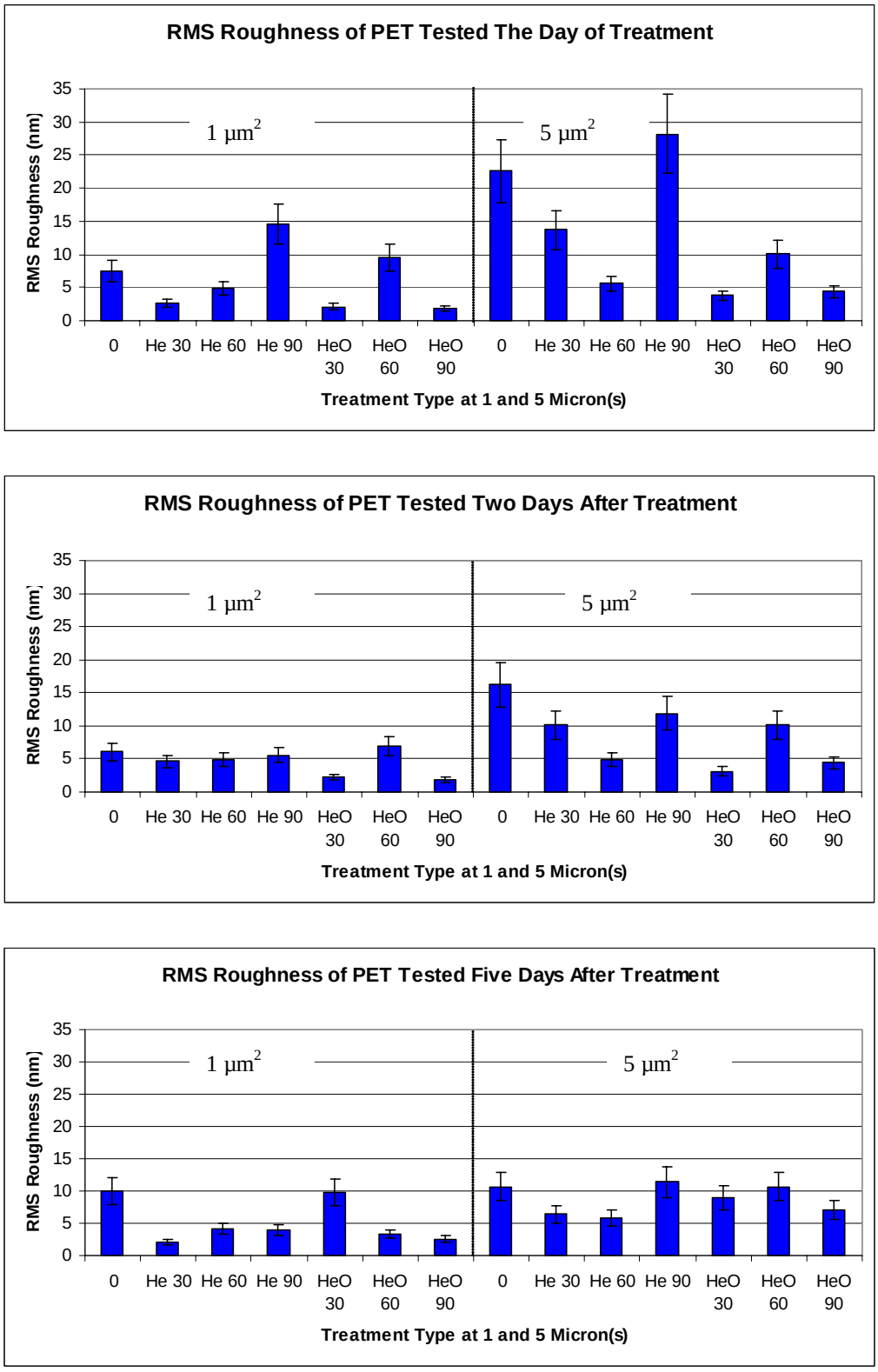

Figure 21: Graphical representation of the root mean square roughness of PET films.

The average roughness of PET treated with both helium and helium/oxygen plasma at a 1 μm^2 scan area appears to decrease with the exception of the He/O 60 seconds treatment on all days tested and the He/O 30 seconds treatment on day 5. The He 90 seconds treatment tested on the day of treatment appears to be artificially high due to the large white spec seen on the surface of the 3D picture (Figure 14d). This characteristic also appears on the He/O 60 seconds treated film at 5 μm^2 tested on day two and the He 90 seconds treated film at 5 μm^2 tested on day five. This could be a dust particle or piece of dirt on the surface that altered the roughness value. The standard error of the control sample, or untreated PET, was approximately 1 nm at a 1 μm^2 scan area and 2.3 nm at a 5 μm^2 scan area. This yields a 17 % and a 20 % standard error of the detection device at 1 μm^2 and 5 μm^2, respectively. This is applied to all of the roughness values since the sample size was only 1. Testing on the day of plasma treatment revealed a decrease in average roughness in all of the samples except He 90 seconds and He/O 60 seconds at a 1 μm^2 scan area and He 90 seconds at the 5 μm^2 scan area. He/O 30 and 90 seconds treatment have a significant lower average roughness than the untreated PET two days after plasma treatment at the 1 μm^2 scan area versus He 60 seconds and all of the helium/oxygen treatments at the 5 μm^2 scan area. Also, five days after treatment, all treatments, excluding He/O 30 seconds were significantly different than the untreated PET at a 1 μm^2 scan area. At the 5 μm^2 scan area, the average roughness was significantly lower than the untreated PET in the He 30 and 60 seconds treatment and He/O 90 seconds treatments. The overall decrease in average roughness in the samples was the result of the plasma interacting with the surface by etching and possibly scissions. The addition of oxygen into the plasma discharge decreased the roughness in most treatment types. This was due to the oxygen increasing the surface activation of the PET, allowing for

oxygen excited atoms and oxygen ions to further interact with the surface, ablation, and removal of particulates or redeposited radicals, and thus creating a smooth surface. The changes in roughness throughout the days tested are most likely due to bond rotation and interaction with the air and polymer surface.

The root mean square (RMS) roughness was also measured for each treatment type. RMS roughness was different than average roughness because it is the root mean square deviation of the surface from the mean surface level over a specific surface wavelength range. It is typically used to quantify variations in surface elevations and is determined by the following equation (Eq. 8):

$$\mathrm{RMS} = \sqrt{\frac{\sum (Z_i - Z_{\mathrm{avg}})^2}{N}}$$

Eq. 8

where *RMS* is the root-mean-square roughness, Z_i is the *i*th height sample out of *N*, the total samples, and Z_{avg} is the mean height [36]. The RMS roughness for the plasma treated PET typically decreased when compared to the untreated PET. Just as in the average roughness, standard and percent error were calculated and found to be approximately 1.2 nm or 15% and 3.4 nm or 21% at the1 μm^2 and 5 μm^2 scan areas, respectively. With this error applied to the RMS roughness values, all of the values taken the day of plasma treatment were significantly less that the untreated PET except the He/O 60 seconds treatment at a 1 μm^2 scan and He 90 seconds treatment at a 5 μm^2 scan. The significant treatments that were tested two days after plasma treatment were He/O 30 and 90 seconds at a 1 μm^2 scan area and He 30 and 60 seconds and He/O 30, 60, and 90 seconds at a 5 μm^2 scan area. On the fifth day after plasma treatment at the 1 μm^2 scan, all of the treatments except He/O 30 were lower than the control

PET. At the 5 μm^2 scan area, three treatments were significantly higher in RMS roughness: He 90 seconds and He/O at 30 and 60 seconds. The change in RMS roughness was again due to the atoms, ions, and molecules interacting with the surface of the polymer and etching away at the top surface layer. The addition of oxygen into the plasma discharge further increased the degree of etching and created a decrease in RMS roughness for every treatment, except the He 90 seconds treatment. This was due to the etching and then redeposition that occurred during this longer treatment time.

4.4 Cell Growth and Proliferation

4.4.1 Keratinocyte Study

Growth and proliferation of the keratinocytes seeded directly on the treated PET 0, 2, and 5 days after treatment was studied after 0.5, 1, 2, 3, and 6 days of incubation. The growth of the keratinocytes is shown in Figure 22 and the proliferation is shown in Figure 23. The proliferation was calculated by using Equation 6 with the fluorescence at day 0.5 as the reference point.

The growth of the keratinocytes was significantly better on PET, both treated and untreated, versus the polystyrene plate. The cells plated on day 0 and tested day 6 days after plating had significantly higher growth than the cells tested at the other time points. The keratinocytes plated on day 2 and tested 3 days after plating also had significantly higher growth than the cells tested the other days. The growth of the keratinocytes plated on day 5 was significantly higher when they were tested on day 0.5, 3, and 6. The increase in growth of the keratinocytes plated on day 5 could be due to the increased hydrophobicity and decreased roughness of the surface by the fifth day after plasma treatment.

The effect of type of working gas used only minimally changed the growth of the keratinocytes. There was an effect of working gas used for the cells plated day 0 and tested day 2 and 6 with a 60 second plasma treatment. Also, the cells tested on day 3 with a 90 second plasma treated surface had a significant difference in the growth. The cells plated on day 2 and tested on day 2 were significantly affected by the gas used for a 30 second treatment. Also, testing the cells on day 0.5, 2, and 3 showed a significant difference in growth on He 90 and He/O 90 treated PET. There was again no observable difference in the growth of the keratinocytes plated on day 5 when comparing the two types of gas plasmas used.

At day 0, the cells appeared to be proliferating by the sixth day of testing and by the third day of testing when the cells were plated on day 2. The cells plated 5 days post plasma treatment appear to be proliferative on the He 60 seconds surface and on all of the plasma treated surfaces by testing 6 days after plating. On a whole, however, minimal differences in growth and proliferation of the keratinocytes on the plasma treated PET were observed.

(a)

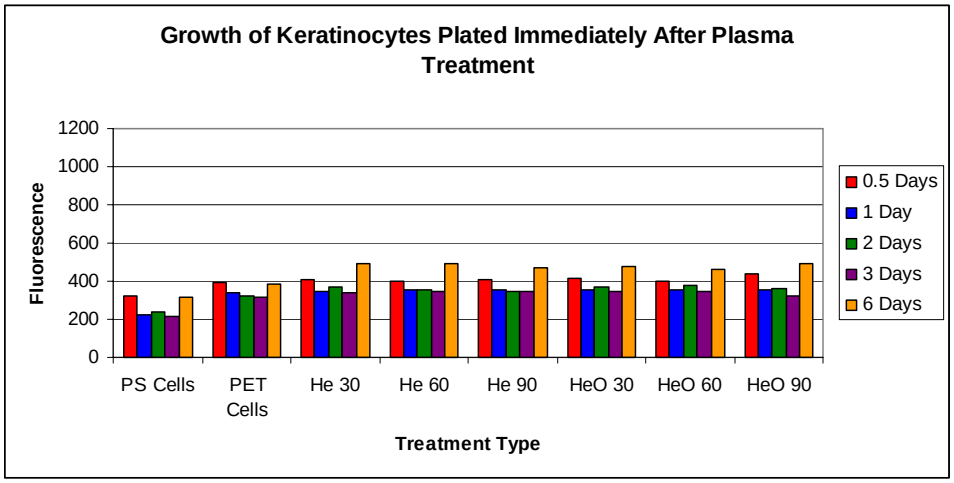

(b)

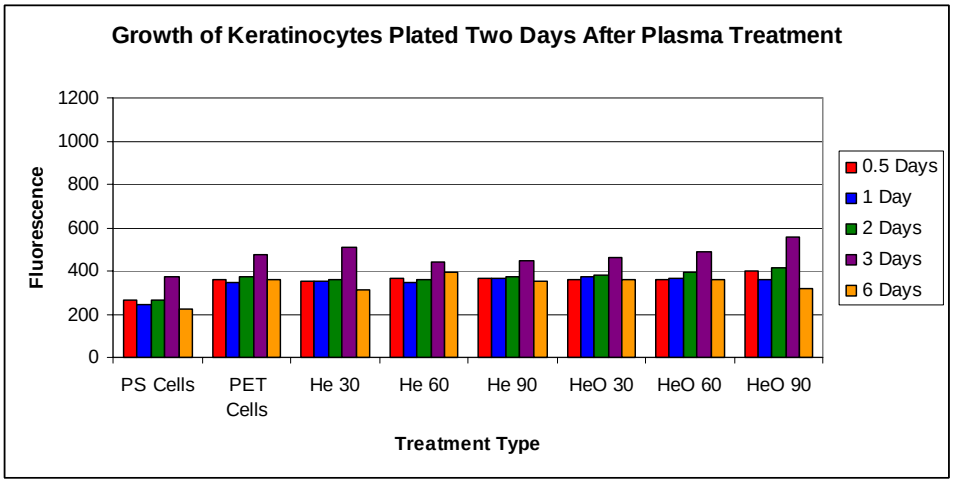

(c)

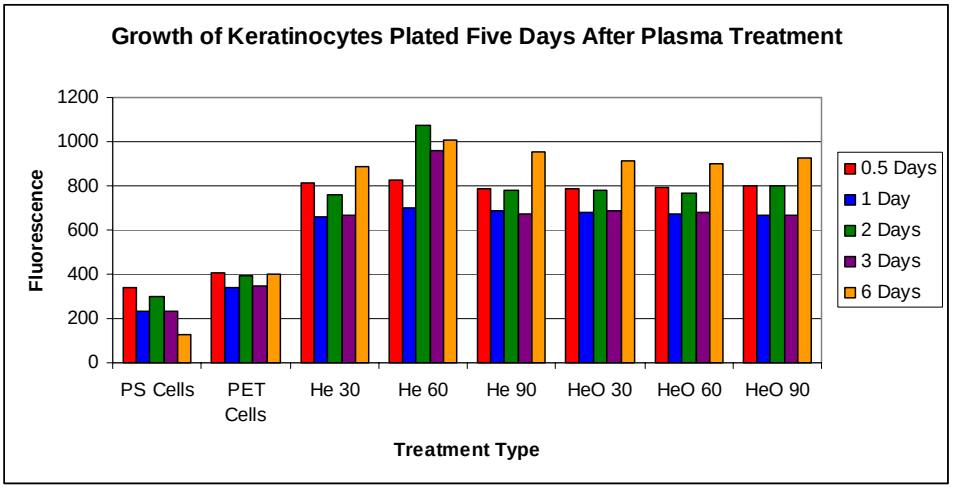

Figure 22: Growth of Keratinocytes Plated (a) Immediately, (b) Two Days, and (c) Five Days After Plasma Treatment

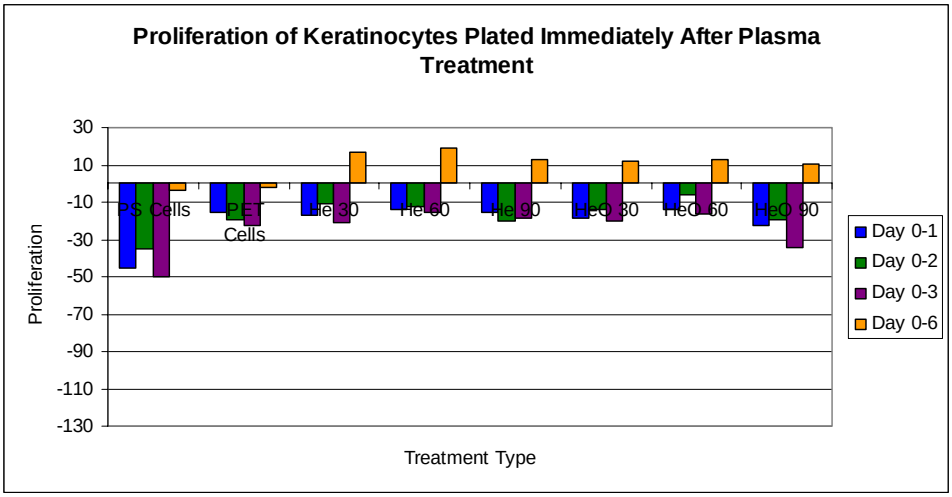

(a)

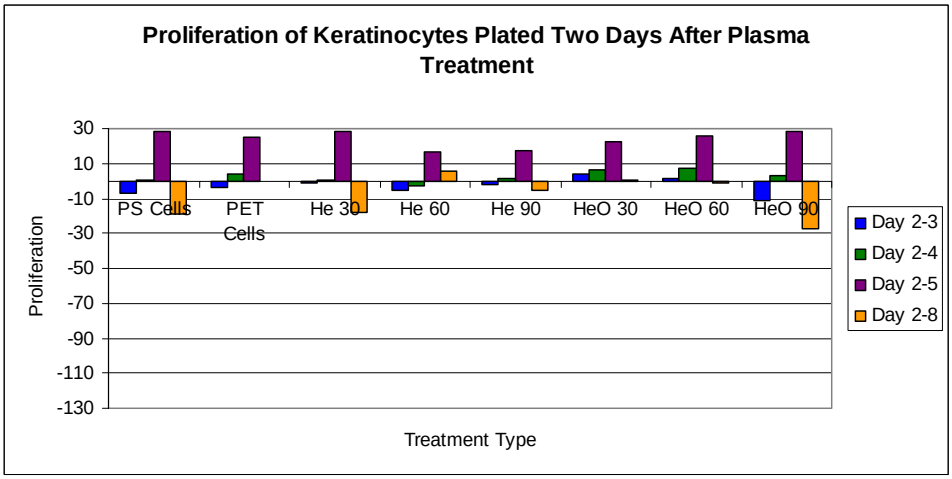

(b)

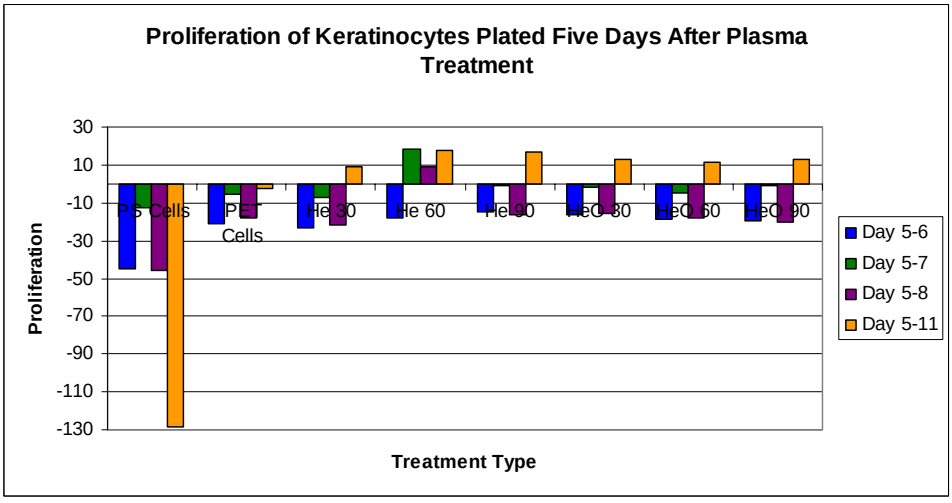

(c)

Figure 23: Proliferation of Keratinocytes Plated (a) Immediately, (b) Two Days, and (c) Five Days After Plasma Treatment

4.4.2 Hepatocyte Study

Growth and proliferation of the hepatocytes seeded directly on the treated PET 0, 2, and 5 days after treatment was studied after 0.5, 1, 2, 3, and 6 days of incubation as shown in Figures 24 and 25, respectively. The proliferation was calculated using the same method as described in the keratinocyte study section.

For all treatments and plating days, the growth of the hepatocytes was significantly higher on PET surfaces versus the polystyrene plates. The growth of the hepatocytes plated immediately after plasma treatment was not affected by the plasma treated surfaces except for those tested on day 2. The cells plated two days after plasma treatment and tested day 0.5 and 2had significantly higher growth over those tested on days 1 and 3. By day 6, the hepatocyte growth had decreased, indicating that they needed to be passaged. The hepatocytes tested 3 days after plating and plated 5 days after plasma treatment also grow significantly better than those tested on the other days.

The type of gas used to plasma treat the surface of the PET did not significantly change the growth or proliferation of the hepatocytes. There was an effect of helium vs helium/oxygen treatment only on the cells plated 5 days after treatment and tested 2, 3, and 6 days after plating. There was also no effect of treatment time on the growth of the hepatocytes.

The proliferation of the hepatocytes does not look very promising except for cells plated 5 days after plasma treatment. These cells were proliferating and appear to prefer the plasma treated surfaces over the untreated PET surface.

(a)

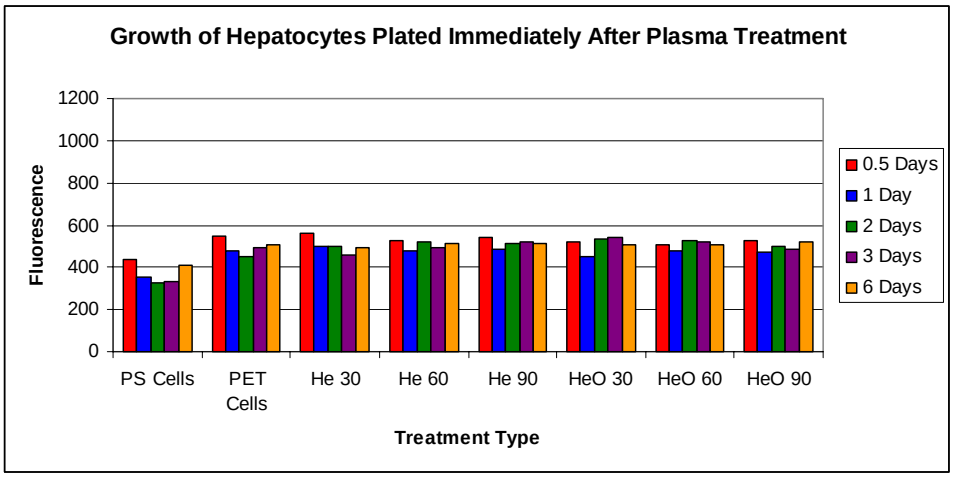

(b)

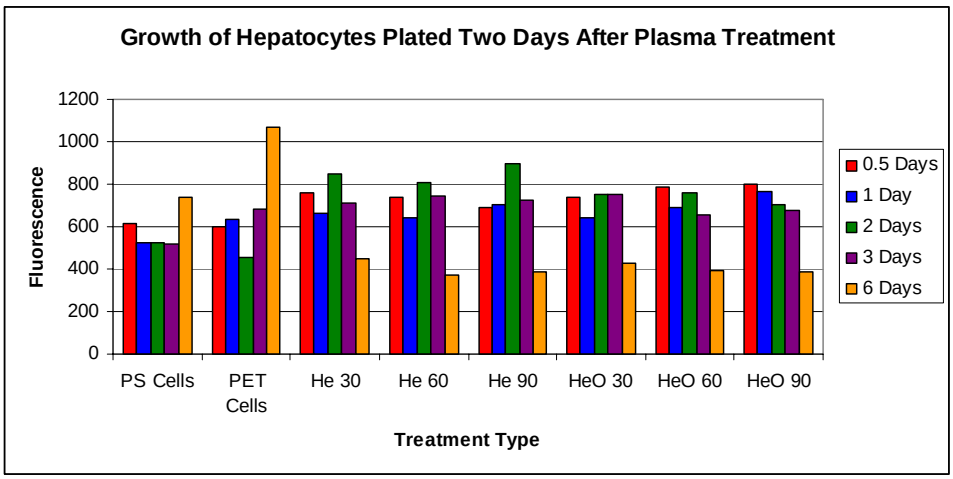

(c)

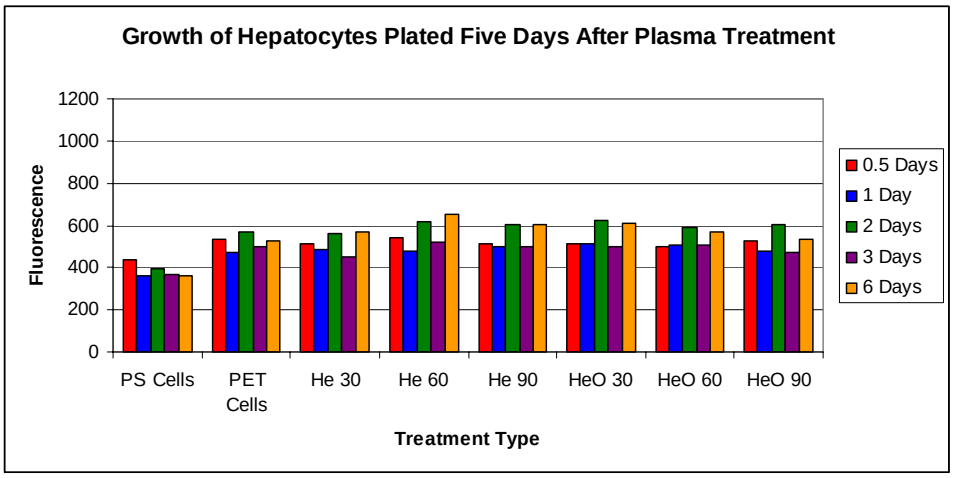

Figure 24: Growth of Hepatocytes Plated (a) Immediately, (b) Two Days, and (c) Five Days After Plasma Treatment

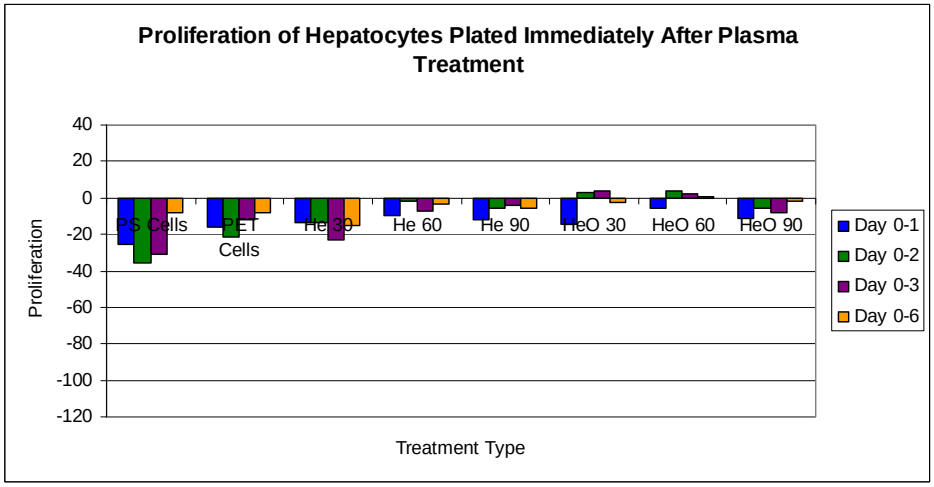

(a)

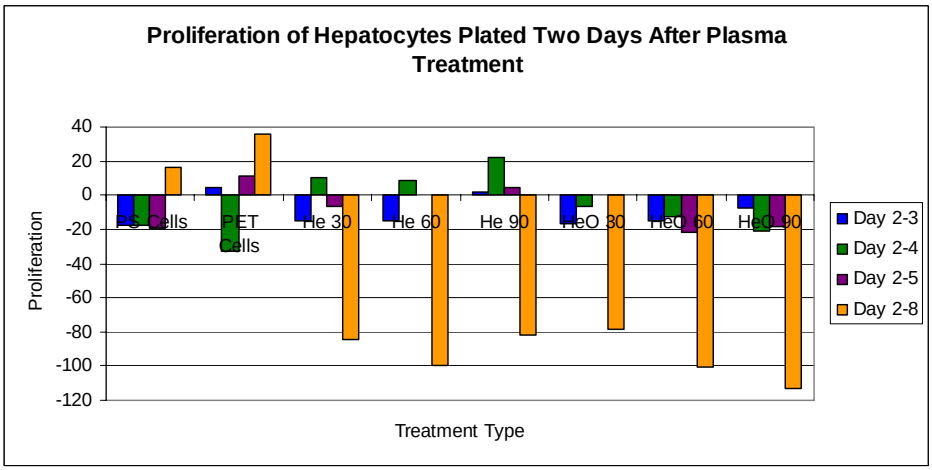

(b)

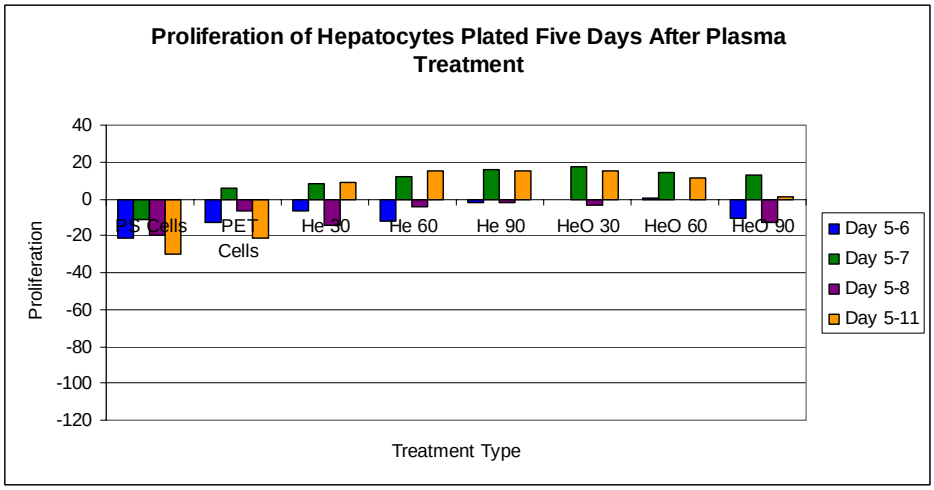

(c)

Figure 25: Proliferation of Hepatocytes Plated (a) Immediately, (b) Two Days, and (c) Five Days after Plasma Treatment

4.5 Cell Adhesion

4.5.1 Keratinocyte Study

The adhesion of keratinocytes to the plasma treated PET was quantified using Equation 7 and is shown in Figure 26. In general, for the cells plated immediately after plasma treatment, the highest adhesion rates occur closest to plating time. On day 6, the cells were not well adhered to the surface of the PET and only approximately 60% of the cells remained on the surface after centrifugation. This was possibly due to the proliferation of the keratinocytes on day 6 and the culture was overly crowded, inhibiting cell adhesion. There was also no significant effect of the plasma treatment types on cell adhesion on the PET. The keratinocytes plated two days after plasma treatment had slightly lower adhesion rates than those plated immediately after plasma treatment. The adhesion was significantly lower on testing day 2 compared to the other testing days. Also, the adhesion on testing day 3 and 6 was consistently higher than those tested on the other days. In general, the cells preferred the surface of the untreated PET over the plasma treated PET, with the exception of the He 60 seconds treatment tested at day 3. The keratinocytes plated five days after plasma treatment had the highest adhesion over the other two plating days. This may be because the surface chemistry of the PET at day 5 was more hydrophobic than the surface at day 0. Overall, the cells on plasma treated PET adhered significantly better than the cells plated on untreated PET. Again, the cells adhered the least when tested on day 2, however for many of the treatments, the percent adhered was over 90%. This indicates that the keratinocytes had good cell-surface interactions and were able to adhere to the PET surface.

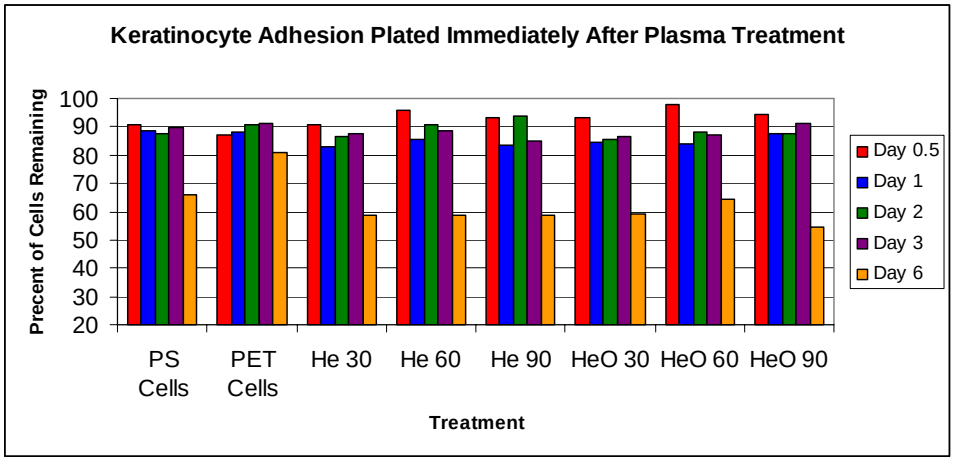

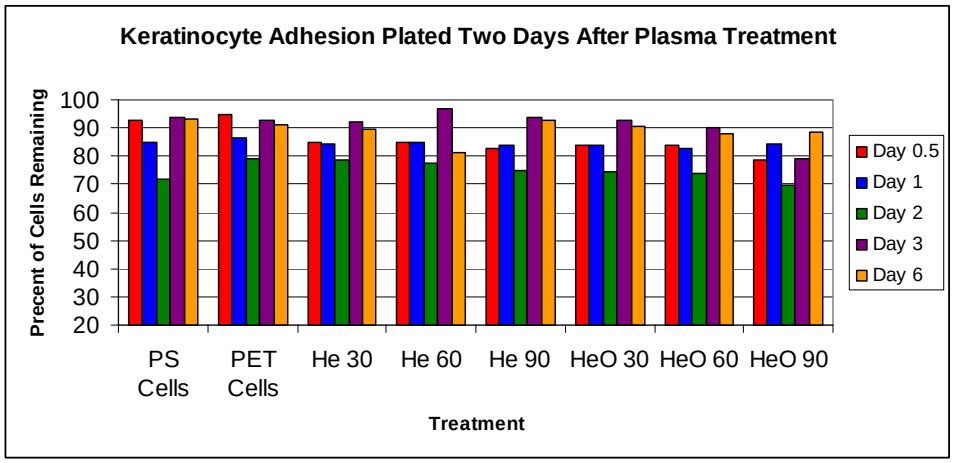

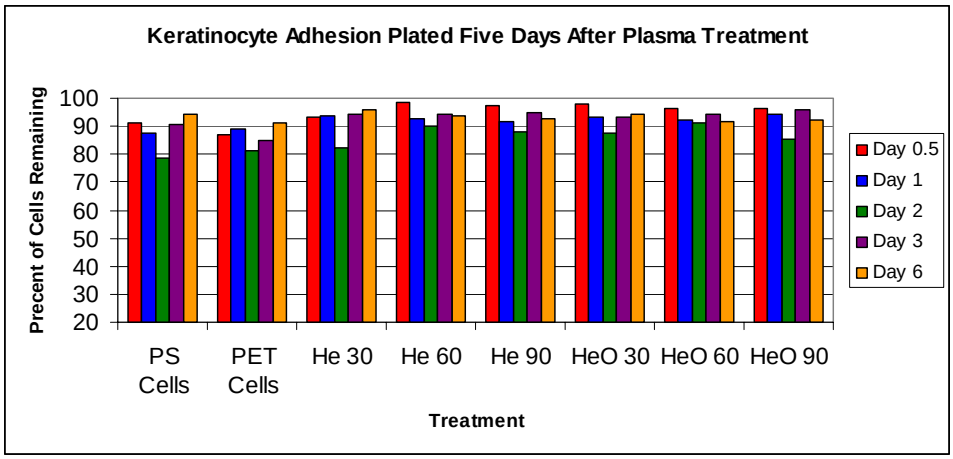

Figure 26: Keratinocyte Adhesion Plated (a) Immediately, (b) Two Days, and (c) Five Days After Plasma Treatment.

4.5.2 Hepatocyte Study

The adhesion of the hepatocytes to the plasma treated PET was quantified using Equation 7 and is shown in Figure 27. Again, there was no statistical significance between treatment types and the adhesion of the hepatocytes on PET. Also, the cells plated five days after plasma treatment adhered better than those plated immediately after plasma treatment, which adhered better than the cells plated two days after plasma treatment. This could be due to the aging effect of the surface chemistry of the PET. The cells plated immediately after plasma treatment surprisingly adhered better to the polystyrene surface than the PET surface. This observation was also found in the adhesion of hepatocytes plated 2 days and 5 days post plasma treatment. Even though the cells were adhering to this surface, they were not proliferating, which means that the cells did not like the surface. The hepatocytes plated two days after plasma treatment appeared to have greatest adhesion when tested at day 2. Also, the cells prefer the untreated PET surface to the plasma treated PET surface, excluding the results of day 6. The hepatocytes plated five days after plasma treatment did not appear to have any significant differences in adhesion of the cells to the different plasma treated surfaces. The cells had a slightly higher adhesion when tested on day 0.5, 1 and 3. Overall, the hepatocytes appeared to prefer the surface chemistry to be slightly hydrophobic, with a contact angle of approximately 67°. This was observed in the indistinguishable differences when the cells were plated 5 days after plasma treatment and the surface contact angle has reached the plateau maximum value.

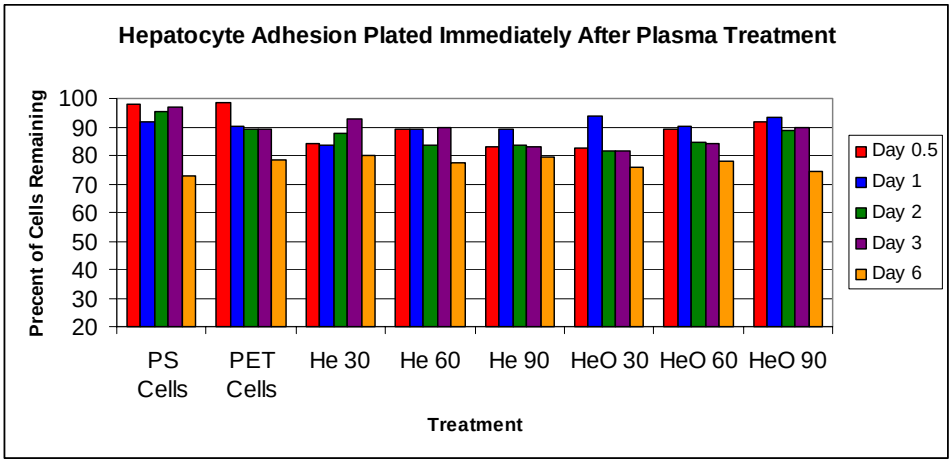

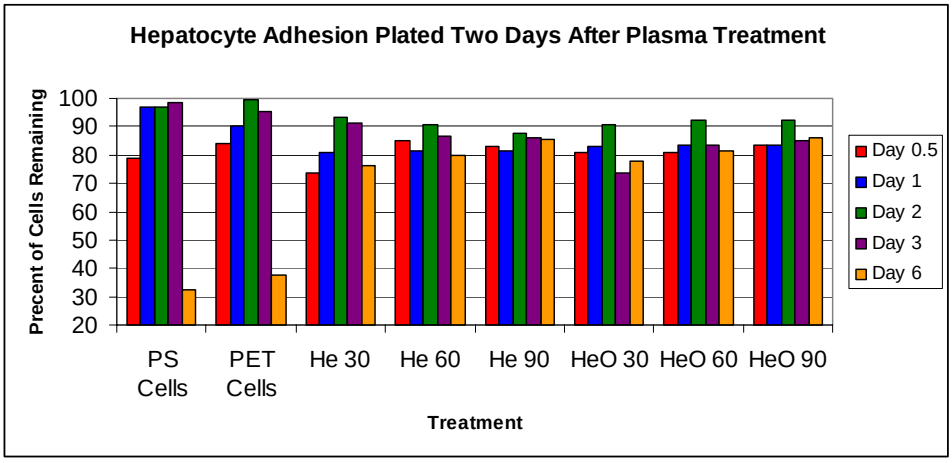

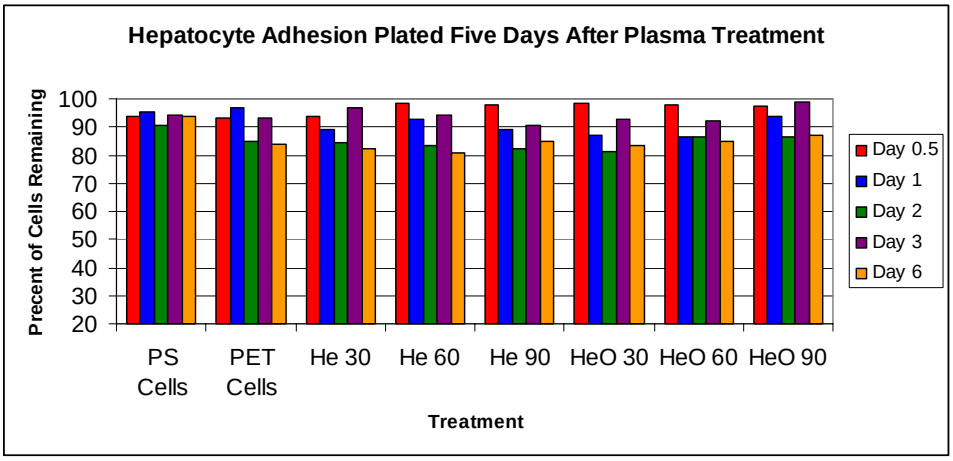

Figure 27: Hepatocyte Adhesion Plated (a) Immediately, (b) Two Days, and (c) Five Days After Plasma Treatment

V. CONCLUSION

This work determined that surface treatment of PET films by plasma discharge only minimally changes keratinocyte and hepatocyte growth, proliferation, and adhesion. The helium plasma discharge increased surface hydrophilicity and the addition of oxygen into the discharge further increased this surface phenomenon. The serum protein, however, in the media further inadvertently altered this chemical surface change. These proteins attached to the surface of the PET which then regulated cell attachment. The antistatic property of the PET was not altered due to plasma treatment and the roughness of the surface was inconclusive because of the large standard error seen on control samples. Visually, however, the surface of the helium/oxygen plasma treated films appeared smoother than the helium plasma treated PET films. The growth, proliferation, and adhesion of porcine keratinocytes plated on plasma treated PET was minimally changed. The growth proliferation and adhesion of the cells on the surface did not appear to be governed by the changes in surface chemistry and morphology caused by plasma treatment. Similar results were found with murine hepatocytes plated on the plasma treated PET. The minimal changes were possibly due to protein adhesion on the surface from the media used. Also, the changes in topography of surface could be undetected by the cells, thus showing that the surface chemistry has more of an effect on cell behavior than nanoscale surface roughness changes.

VI. FUTURE WORK

Investigations into the effect of protein absorption on the surfaces of plasma treated PET needs to be performed. The media caused significant changes in the surface chemistry and the protein adherence to the surface altered the cell behavior and interfering with the growth, proliferation, and adhesion of the cells.

Additional data points need to be collected for the average roughness and root mean square roughness values. Only one data point was used in this study; however, to properly determine significance of the values, a sample size of four is recommended.

To further expand the knowledge of how surface chemistry and topography influence cell behavior, other adherent cell types should be tested on plasma treated PET, as well as other polymers. For example, cells that could be tested include, but are not limited to endothelial cells, epithelial cells, and/or fibroblasts. Some examples of polymer surfaces that would be interesting to modify using plasma discharge include polypropylene, polyvinyl alcohol, and/or polymethyl-methacrylate.

REFERENCES

[1] Chi-Ming Chan, *Polymer Surface Modification and Characterization*, Hanser/Gardner Publications, Inc., New York (1994).

[2] Witold Rakowski, M. Okoneiwski, K. Bartos, and J. Zawadzki, "Plasma treatment of textiles-potential applications and future prospects," *Melliand Textilberichte[English Edition]*, 301 (April 1982

[3] Dennis M. Manos and Daniel L. Flamm, Ed., *Plasma Etching: An Introduction*, Academic Press, Inc., San Diego, 1989

[4] Lanza RP, Langer R, and Vacanti J. *Principles of Tissue Engineering*. Academic Press, Inc., San Diego, 2000.

[5] Hjortso MA and Roos JW. *Cell Adhesion: Fundamentals and Biotechnological Applications*. Marcel Dekker, Inc., New York, 1995.

[6] Leigh IM, Lane EB, and Watt FM. *The Keratinocyte Handbook.* Cambridge University Press, New York, 1994.

[7] Alberts B, Johnson A, Lewis J, Raff M, Roberts K, and Walter P. *Molecular Biology of the Cell*. Garland Science, New York, 2002.

[8] Kreis T and Vale R. *Guidebook to the Extracellular matrix, Anchor, and Adhesion Proteins*. Oxford University Press, Inc., New York, 1999.

[9] Gupta B, Plummer C, Bisson I, Frey P, and Hilborn J. *Biomaterials*, 23, 863 (2002).

[10] Jansen JA, van der Waerden JPCM, and de Groot K. *Biomaterials*, 10, 604 (1989).

[11] Dewez JL, Doren A, Schneider YJ, and Rouxhet PG. *Biomaterials*, 20, 547 (1999).

[12] Loh IH. Plasma surface modification in biomedical applications. *AST Technical Journal*. http://www.astp.com/PDFs/PS_biomed.pdf.

[13] Yubing X, Sproule T, Li Y, Powell H, Lannutti JJ, Kniss DA. *Journal of Biomedical Materials Research*, 61(2), 234, (2002).

[14] Gniadecki R. *General Pharmacology*, 30(5), 619 (1998).

[15] Moustafa M, Simpson C, Glover M. *Diabetic Medicine*, 21(7), 786 (2004).

[16] Eves PC, Beck AJ, Shard AG. *Biomaterials*, 26(34), 7068 (2005).

[17] Haddow DB, Steele DA, Short RD. *Journal of Biomedical Materials Research Part A*, 64A(1), 80 (2003).

[18] Wagner WR, Muzzio DJ, Rilo HR, Deglau T, Ataai MM, Michalopoulos GK, and Block GD. *Tissue Engineering*, 3(3), 289 (1997).

[19] Geckeler KE, Gebhardt R, and Grünwald H. *Naturwissenschaften*, 84, 150 (1997).

[20] Krasteva N, Groth TH, Fey-Lamprecht F, and Altankov G. *Journal of Biomaterials Science Polymer Edition*, 12(6), 613 (2001).

[21] Carlisle ES, Mariappan MR, Nelson KD. *Tissue Engineering*, 6(1), 45 (2000).

[22] Allen DG, Riviere JE, and Monteiro-Riviere NA. *Toxicology Letters*, 119, 209 (2001).

[23] Clark JB, Rice L, Sadiq T, Brittain E, Song L, Wang J, and Gerber DA. *Biochemical and biophysical Research Communications*, 329, 337 (2005).

[24] Seglen PO. *Methods in Cell Biology*, 13, 29 (1976).

[25] Matthews SR, Hwang Y, McCord MG, and Bourham MA. *Journal of Applied Polymer Science*, 94(6), 2383 (2004).

[26] Roth JR, Sherman DM, Gadri RB, Karakaya F, Chen A, Montie TC, Kelly-Wintenberg K, and Tsai PP-Y. *IEEE Transactions in Plasma Science*, 28(1), 56 (2000).

[27] Laroussi M, Alexeff I, Richardson JP, and Dyer FF. *IEEE Transactions in Plasma Science*, 30(1), 158 (2002).

[28] Bures BL, Donohue KV, Roe RM, and Bourham MA. *IEEE Transactions in Plasma Science*, 33(1), 290 (2005)

[29] Bures BL, Ph.D. dissertation, NCSU (2004).

[30] Yasuda T and Okuno T. *Langmuir*, 10, 2435 (1994).

[31] Hartland S. *Surface and Interfacial tension: Measurement, Theory, and Applications*. Marcel Dekker, Inc., New York, 2004.

[32] ASTM International, D 5946-04.

[33] Morris WT. *Plastics & Polymers*, 41 (1970)

[34] Ballou JW. *Textile Research Journal*, 146 (1954).

[35] Müller B, Riedel M, Michel R, DePaul SM, Hofer R, Heger D, and Grutzmacher D. *Journal of Vacuum Science and Technology*, 19(5), 1715 (2001).

[36] Yoshida W and Cohen Y. *Journal of Membrane Science*, 215, 249 (2003).

APPENDIX A – TABULATED DATA

Day	0	He 30	He 60	He 90	HeO 30	HeO 60	HeO 90
15 minutes	69	46.5	42.5	39.25	42.75	42.5	39.5
1	69.25	57.25	52.25	43	48.75	48.25	49.75
2	69.75	59.75	55.5	50	50	55.25	46.75
3	69.5	61.25	59.75	59	56.5	54.5	60
4	68.5	63	61.25	55.5	54.25	61.75	58.5
5	68.75	66	64.25	59.25	59.25	63	61.5
6	68.5	64.25	64	61.75	61.75	64	63
7	68.25	65	65.25	62	63.5	61.75	65.5
8	68.5	66.5	65.5	63	63.75	63.75	62.5
9	69.25	67	62.5	60	62.5	60.5	63.25
10	68.5	64.5	66.25	58.25	60	58.75	62.5

Table 1: Average Contact Angle of Films Stored in Air at Room Temperature.

Day	0	He 30	He 60	He 90	HeO 30	HeO 60	HeO 90
15 minutes	65.5	42.25	35.25	35.5	45.25	41.75	42
1	66.75	57.75	53.75	44.75	49.25	44.75	43
2	68.25	55.5	56.75	57.25	56	57.5	57
3	68.75	57	61.25	59.5	57.25	56.75	60
4	69	57.75	61	60.5	58.25	58.75	58
5	70.5	60.75	61.75	63	61.5	61	61.25
6	69.5	61.5	62	60.25	61.5	60.75	62.5
7	70.5	59.75	59.75	60.5	60.75	61.25	61.25
8	69.5	61.5	60.5	60.5	58.25	62.5	59
9	66.25	59.75	59.75	60.75	60.75	60	61
10	67.75	58.5	60.75	60.75	60.75	58	58.5

Table 2: Average Contact Angle of Films Stored in a Freezer.

Day	0	He 30	He 60	He 90	HeO 30	HeO 60	HeO 90
15 minutes	64.5	62.5	53	57.75	61	52.5	55
1	46	46.75	48.75	38	48.75	39.25	46.5
2	58.5	55.25	55.25	50.25	54.5	48.75	50.5
3	61.5	53.5	54	54.5	54.75	54	54.25
4	64.5	56.5	56.5	51.25	57.75	54	55
5	61.75	55	54.75	52	60.75	53.25	53.5
6	58.5	57.75	59.5	54.75	56	54.75	57.5
7	62	56.5	58.25	56	58.5	56.75	58
8	56.5	56.75	55.25	58	58	54.75	54.75
9	56.75	55.75	60	55	56.75	54	55.5
10	64.25	54	56.5	57.5	55	56	57.25

Table 3: Average Contact Angle of Films Stored in Keratinocyte Media.

Day	0	He 30	He 60	He 90	HeO 30	HeO 60	HeO 90
15 minutes	60.5	51	60.75	60.25	60.25	53.5	55
1	54.75	51.5	54.75	54.25	50.5	35.75	33
2	54.5	49.5	53.5	51.75	47.75	53.75	57
3	53	55.5	60.25	50.5	54.25	55.75	59
4	55	54.5	58.5	51.25	59.5	50.5	55.75
5	50.75	51.25	54	54.25	60	51.75	60.5
6	53.75	53.75	54.75	54	53.5	50.75	59.5
7	55.5	52.75	50	50.25	46.75	50.75	56.25
8	50.75	55	56.25	49.5	47.25	47.75	59
9	53.75	54.5	53.25	56.25	53.75	49.75	54.25
10	62	56.5	59.5	59.75	61.25	55.25	52.75

Table 4: Average Contact Angle of Films Stored in Hepatocyte Media.

	Day Tested After Treatment – 1 µm				Day Tested After Treatment – 5 µm		
Treatment	0	2	5		0	2	5
0	6.06	4.2	7.72		16.3	10.5	8.46
He 30	2.01	3.75	1.7		10.6	8.09	4.61
He 60	4.05	3.81	3.33		4.21	3.86	4.55
He 90	6.82	4.46	3.25		16.6	8.59	6.71
HeO 30	1.54	1.73	7.66		2.69	2.32	6.15
HeO 60	7.73	5.78	2.53		6.34	6.34	8.97
HeO 90	1.38	1.38	1.96		3.05	3.05	5.16

Table 5: Average roughness (nm) of PET films.

	Day Tested After Treatment – 1 µm				Day Tested After Treatment – 5 µm		
Treatment	0	2	5		0	2	5
0	7.51	6.05	9.99		22.6	16.2	10.7
He 30	2.61	4.61	2.11		13.7	10.1	6.4
He 60	4.92	4.88	4.18		5.57	4.9	5.84
He 90	14.5	5.59	4.02		28.2	11.9	11.4
HeO 30	2.11	2.27	9.74		3.75	3.12	8.9
HeO 60	9.51	6.87	3.32		10.1	10.1	10.7
HeO 90	1.83	1.83	2.57		4.39	4.39	7.12

Table 6: Root mean square roughness (nm) of PET films.